H→γγ fiducial and differential cross-section measurements with full Run2 dataset at ATLAS

Fábio Lucio Alves (Nanjing University)
on behalf of the ATLAS Collaboration

中国物理学会高能物理分会第十一届全国会员代表大会暨学术年会
2022年8月8日至11日 大连

Introduction

- **It's 10 years since the Higgs boson discovery (2012):**
  - Measurements of its properties with full Run2 dataset (2015-2018) in excellent agreement with the SM (See Gangcheng's talk)
- **Inclusive and Differential Fiducial Higgs measurements:**
  - Test the SM Higgs boson properties and probe for BSM contributions:
    - measured differential cross-sections distributions are compared to state-of-the-art SM predictions
  - Less model-dependent measurements: small extrapolations and SM assumptions
  - $H \to \gamma\gamma$ channel measurements arXiv:2202.00487:
    - No separation of production modes is aimed
    - Observables sensitive to New Physics, contributions of different Higgs boson production modes, CP-properties and QCD effects
    - Cross-sections measured are used in the interpretation via EFT theory and setting limits on Yukawa bottom- and charm-quarks using di-photon pT shape information

July 2012

July 2022

H→γγ analysis in a nutshell

- ***Signature:*** two reconstructed isolated photons
  - ***diphoton vertex:*** NN algorithm, improves mass resolution
  - ***kinematic selections:***
    - $\mathrm{pT}(\gamma_1) > 0.35 m_{\gamma\gamma}$; $\mathrm{pT}(\gamma_2) > 0.25 m_{\gamma\gamma}$
    - $|\eta| < 2.37$ (exclude 1.37-1.52 region)
    - Jets: pT > 30 GeV, |y| < 4.4
    - $105\ GeV < m_{\gamma\gamma} < 160\ GeV$
  - ***Signal Modelling*:**
    - double-sided Crystal Ball function: MC simulation

- ***Background sources and modelling:***
  - SM $\gamma\gamma$ production (irreducible) and $\gamma - jet$ and $jet - jet$ (reducible ones):
    - built background-only templates, GPR approach to smooth statistical fluctuations in low-yields templates
  - choice of the background model: signal+background fits to $m_{\gamma\gamma}$ background-only templates:
    - function's choice uncertainty ('spurious signal')

Fits to $m_{\gamma\gamma}$ to extract the signal yields

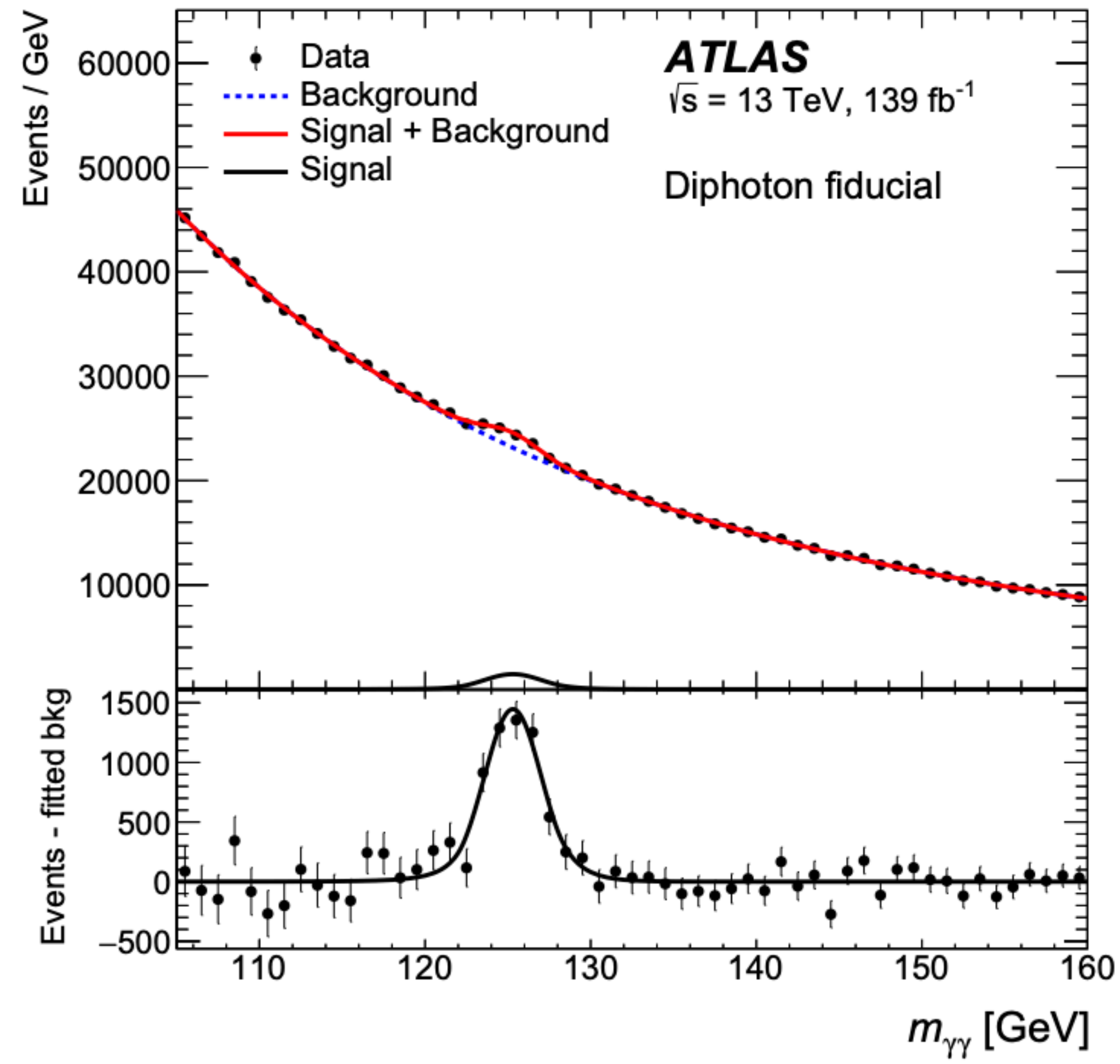

Measurement methodology

- ***Fiducial region:*** defined to closely match the detector-level analysis and object selections
- ***Differential fiducial cross-section*** are measured in bins of the studied observable (bin i of a variable x)
  - ✓ N_i^{sig} ***(measured signal yield):*** extracted signal events in data
  - ✓ Δx ***(bin width):*** choice based on significance (close to or greater than 2σ) and minimize migrations
  - ✓ c_i ***(correction factor):*** accounts for detector inefficiencies and resolutions effects as well as migrations in and out of fiducial region
    - MC response matrix

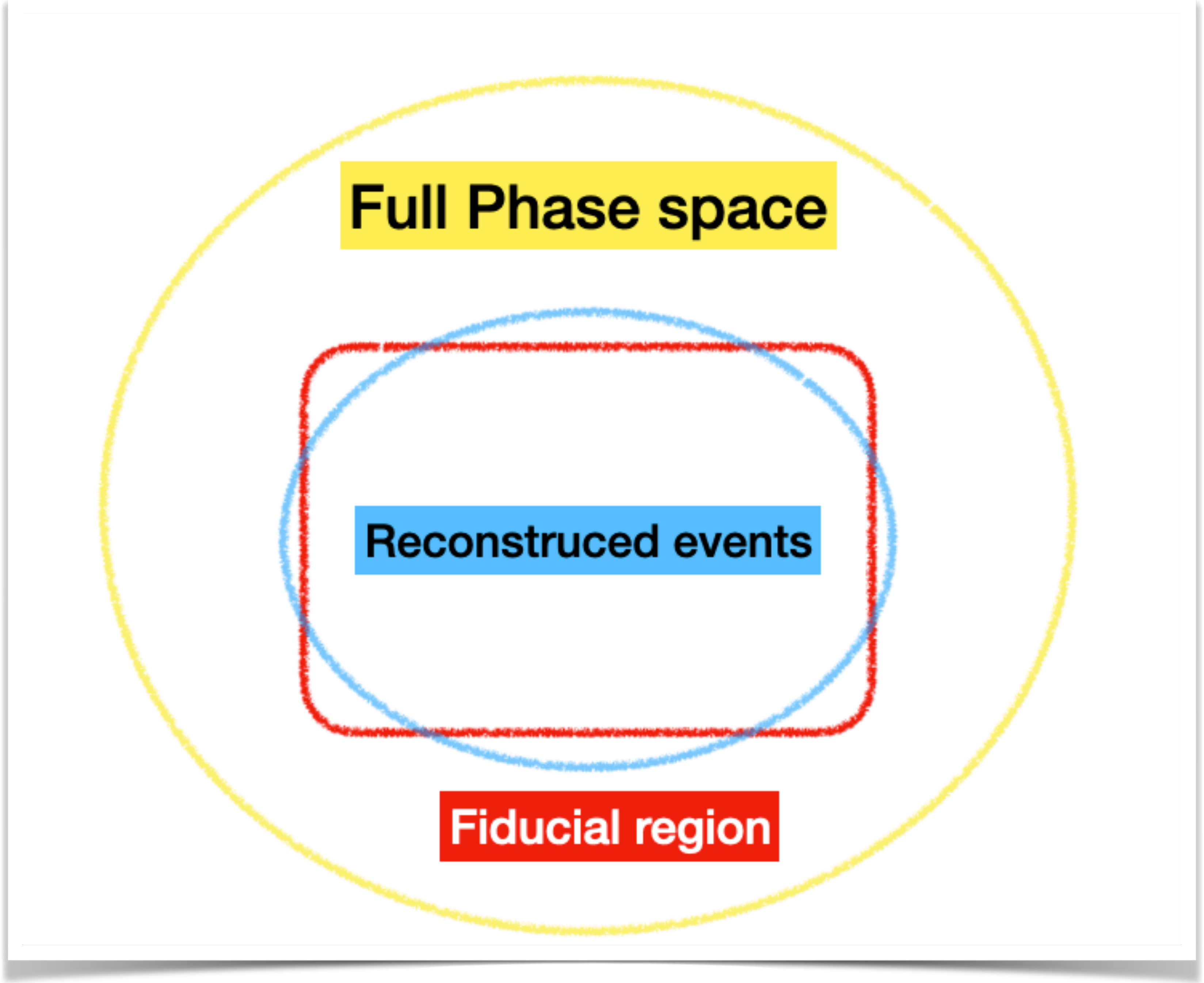

$$\frac{d\sigma_i}{dx} = \frac{N_i^{sig}}{c_i \Delta x \mathscr{L}}$$

Differential fiducial cross-section

Fiducial cross-section measurement

Fiducial cross-sections measurements in regions enriched in various production modes

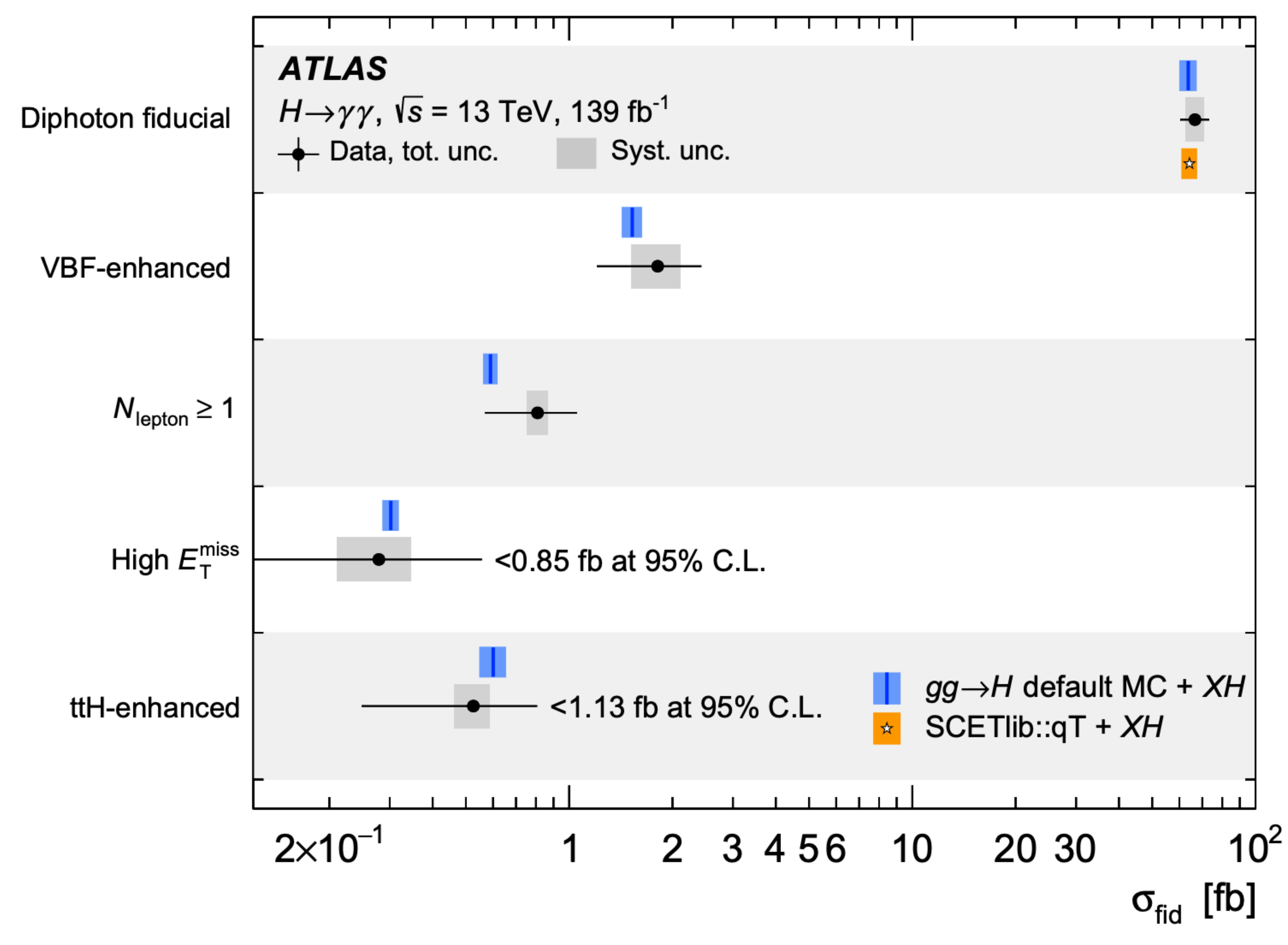

Diphoton fiducial region

Source	Uncertainty [%]
Statistical uncertainty	7.5
Systematic uncertainties	6.4
Background modelling (spurious signal)	3.8
Photon energy scale & resolution	3.6
Photon selection efficiency	2.6
Luminosity	1.8
Pile-up modelling	1.4
Trigger efficiency	1.0
Theoretical modelling	0.4
Total	9.8

Diphoton fiducial cross-section =
$67 \pm 5(stat.) \pm 4(sys.)\ fb$

SM = $64 \pm 4\ fb$

- Measurement is statistical dominated
- Background modelling is the largest systematic uncertainty

Differential cross-section vs $p_T^{\gamma\gamma}$ and $|y_{\gamma\gamma}|$

default MC: Powheg NNLOPS, normalized to N3LO (QCD)+NLO(EW)

- **Low $p_T^{\gamma\gamma}$:** sensitive to bottom- and charm-quark Yukawa couplings
- **High $p_T^{\gamma\gamma}$:** top quark coupling and BSM effects

- $|y_{\gamma\gamma}|$ is sensitive to light-quark Yukawa coupling and gluon distribution in the proton

pT(H) > 350 GeV: sensitivity to BSM effects

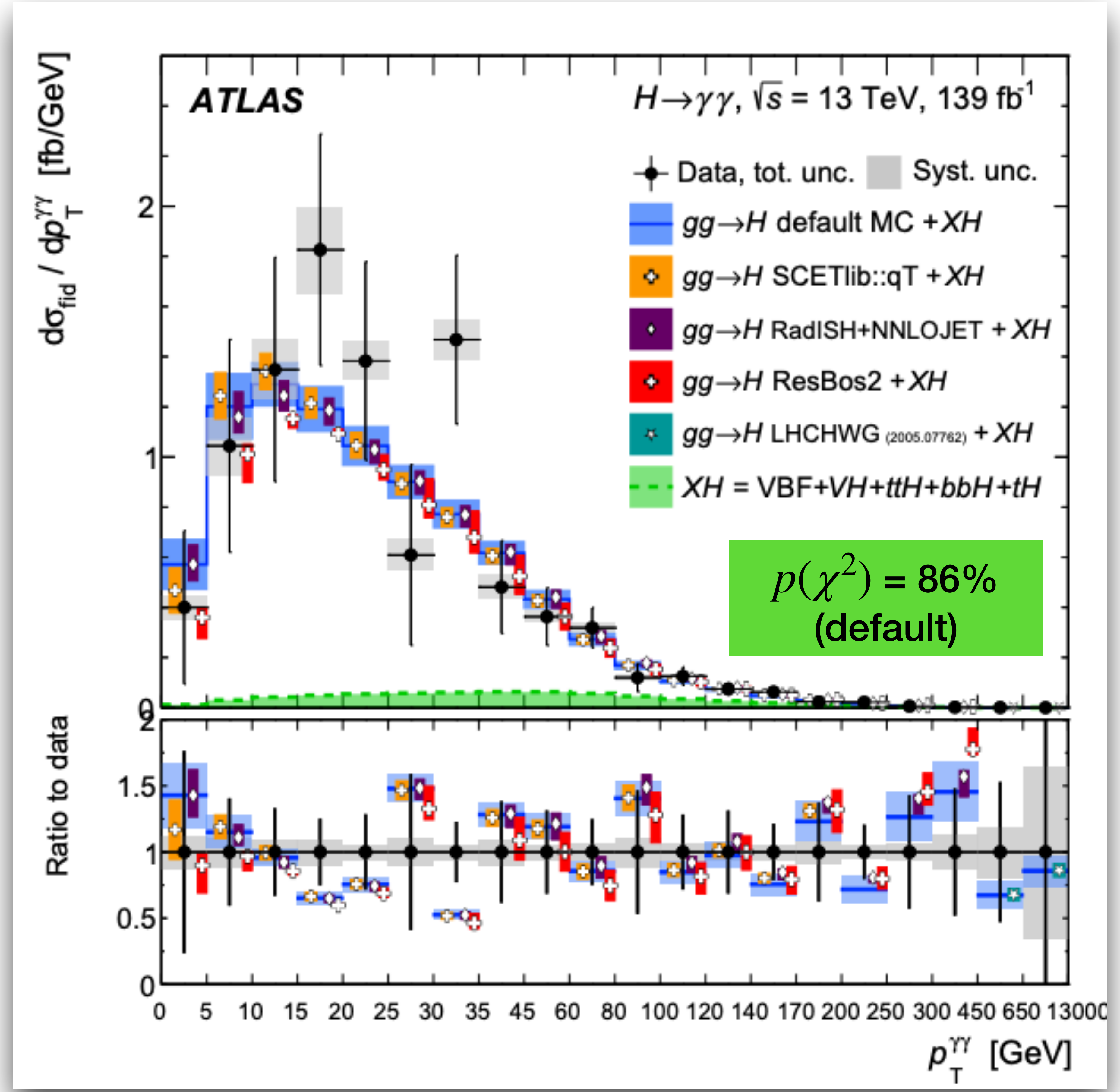

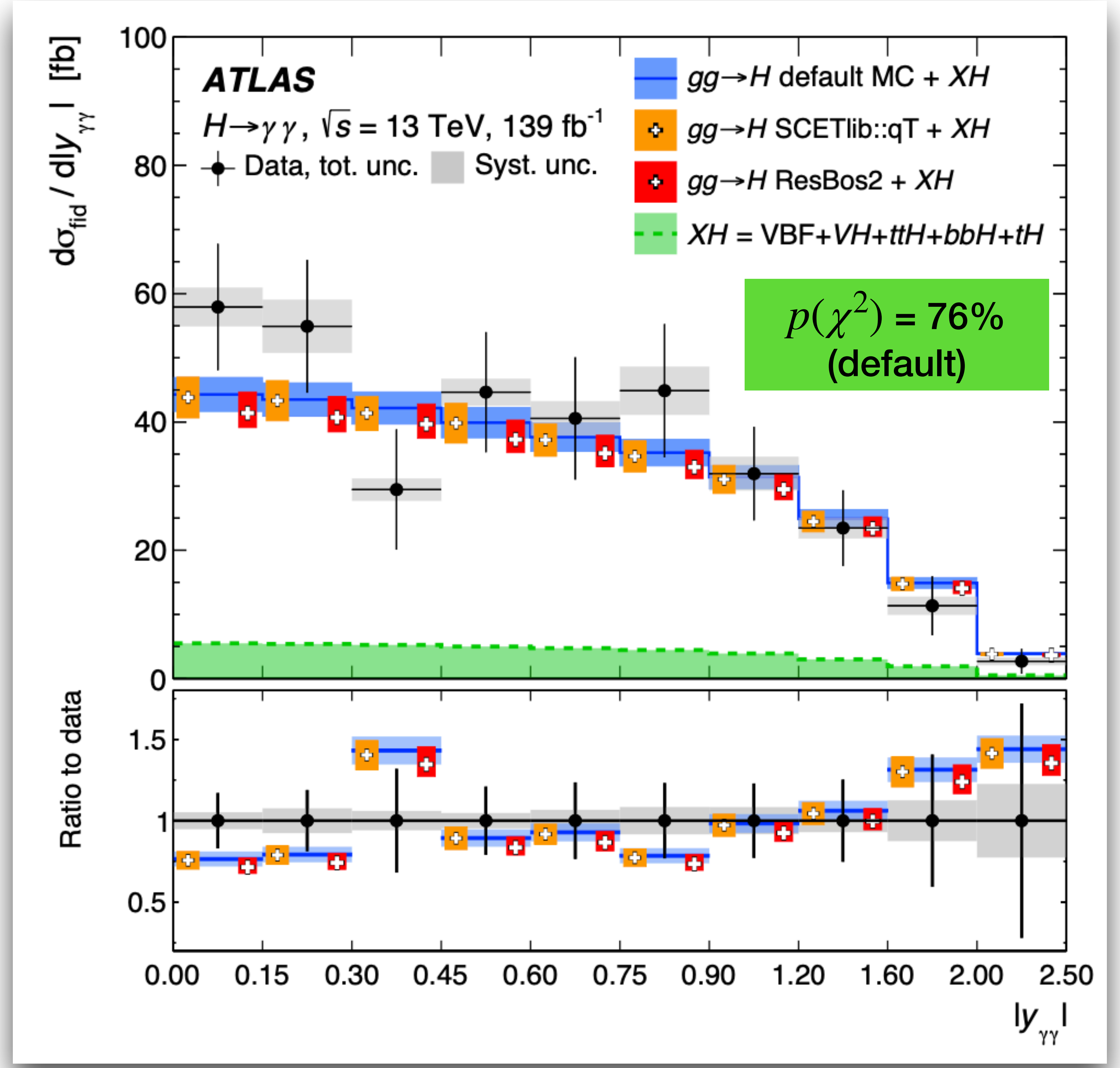

Good agreement with the SM predictions whithin the uncertainties

Cross-section vs N_{jets} and N_{b-jets}

- Inclusive N_{jets} (pT > 30 GeV and $|y| < 4.4$):
  - sensitive to different Higgs boson production modes and QCD modelling (ggF)
- N_{b-jets}: at least 1 central jet and veto on electrons/muons (suppress ttH contribution)
  - sensitive to Higgs production in association with heavy particles

Good agreement with the SM predictions

Jet-related systematic reaching up to 24% in highest jet multiplicities

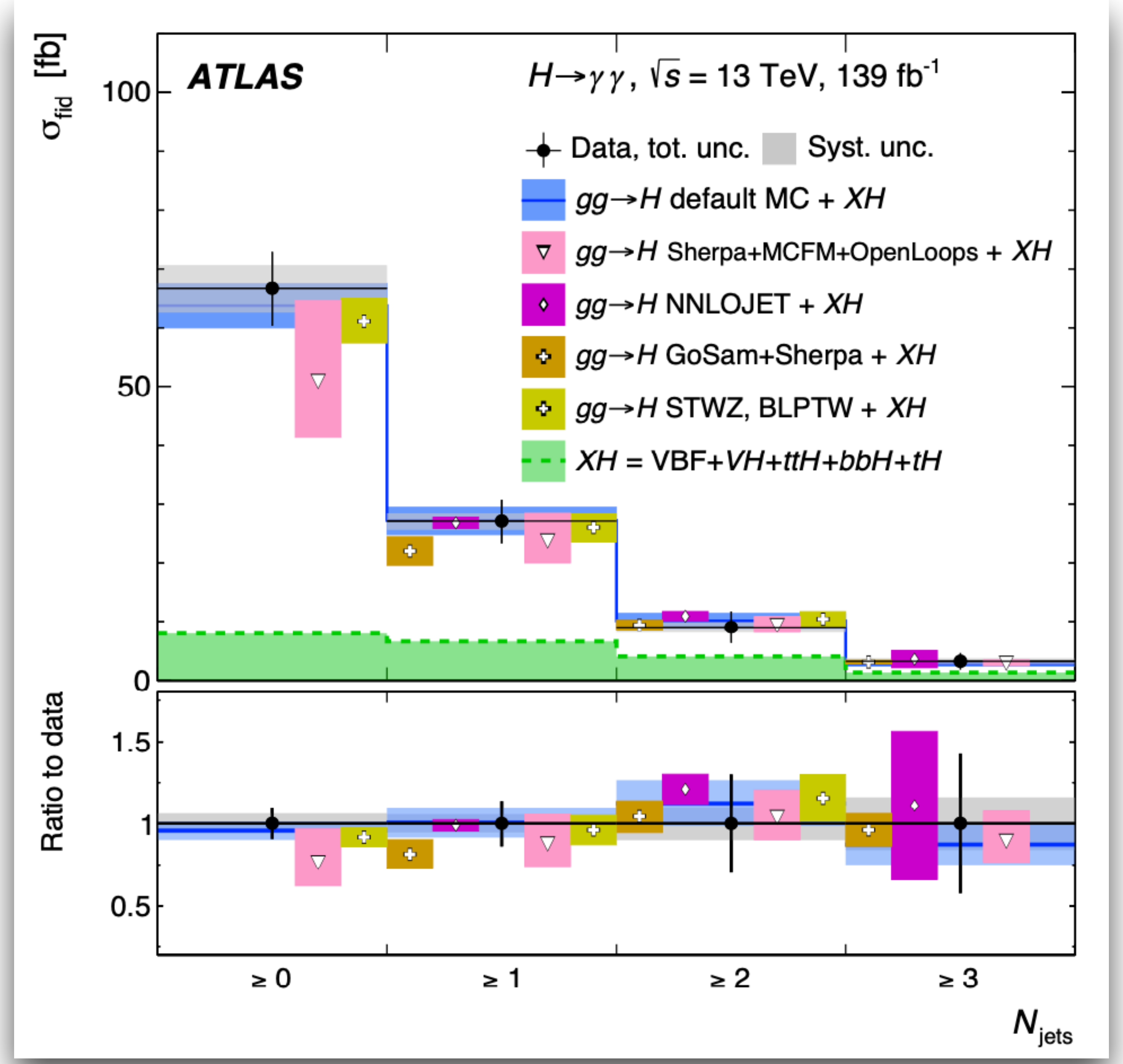

Inclusive N_{jets}
$p(\chi^2)$ = 95%
(default)

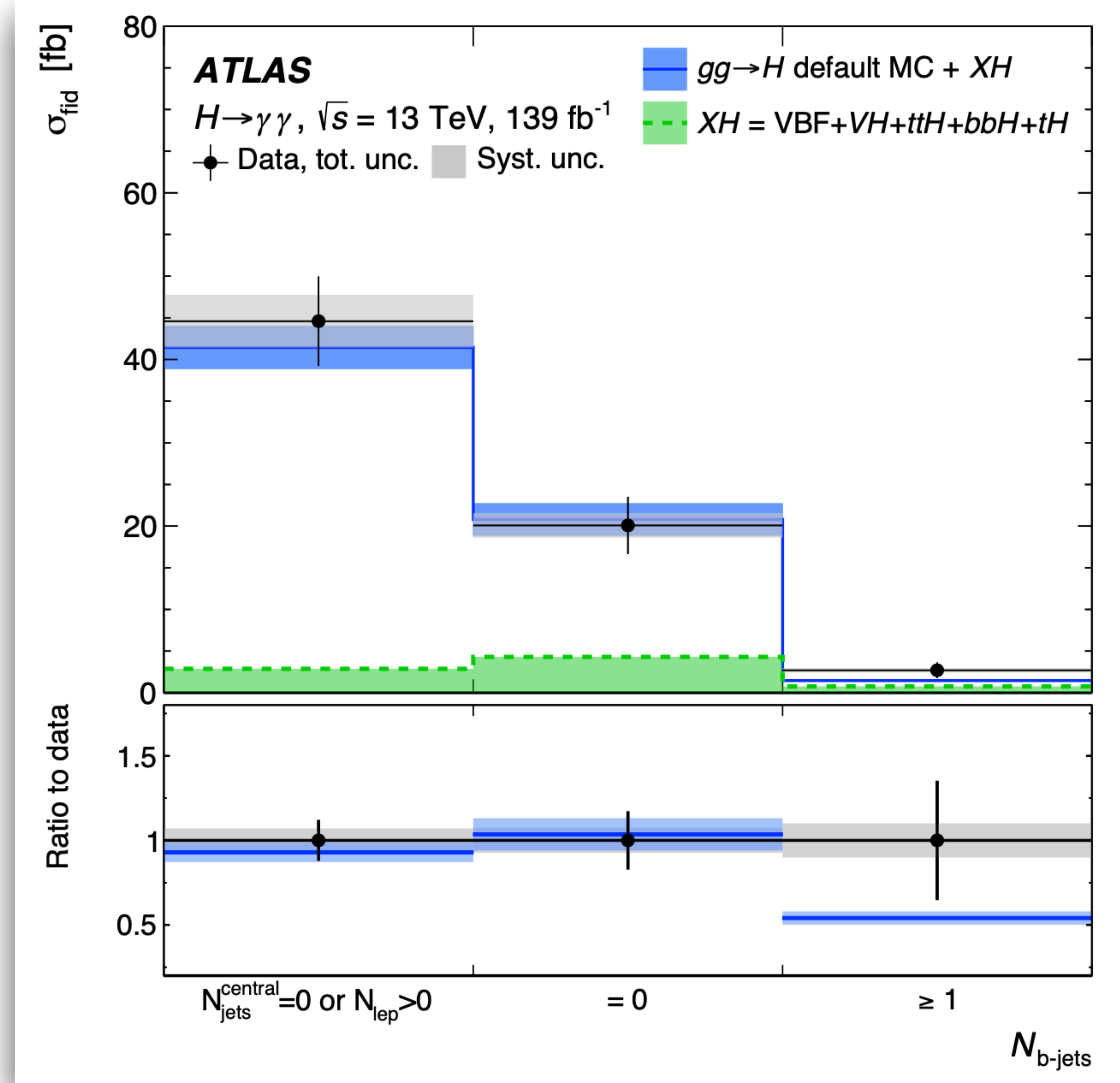

N_{b-jets}
$p(\chi^2)$ = 60%
(default)

Differential cross-section vs p_T^{j1}, m_{jj} and $\Delta\phi_{jj}$

- p_T^{j1}: same range as $p_T^{\gamma\gamma}$ but within coarser bins at low pT
  - $p(\chi^2) = 78\%$ (default MC)

- m_{jj} : highest bin is most sensitive to the VBF production mechanism
  - $p(\chi^2) = 79\%$ (default MC)

- $\Delta\phi_{jj}$: sensitive to CP properties of the Higgs boson
  - $p(\chi^2) = 91\%$ (default MC)

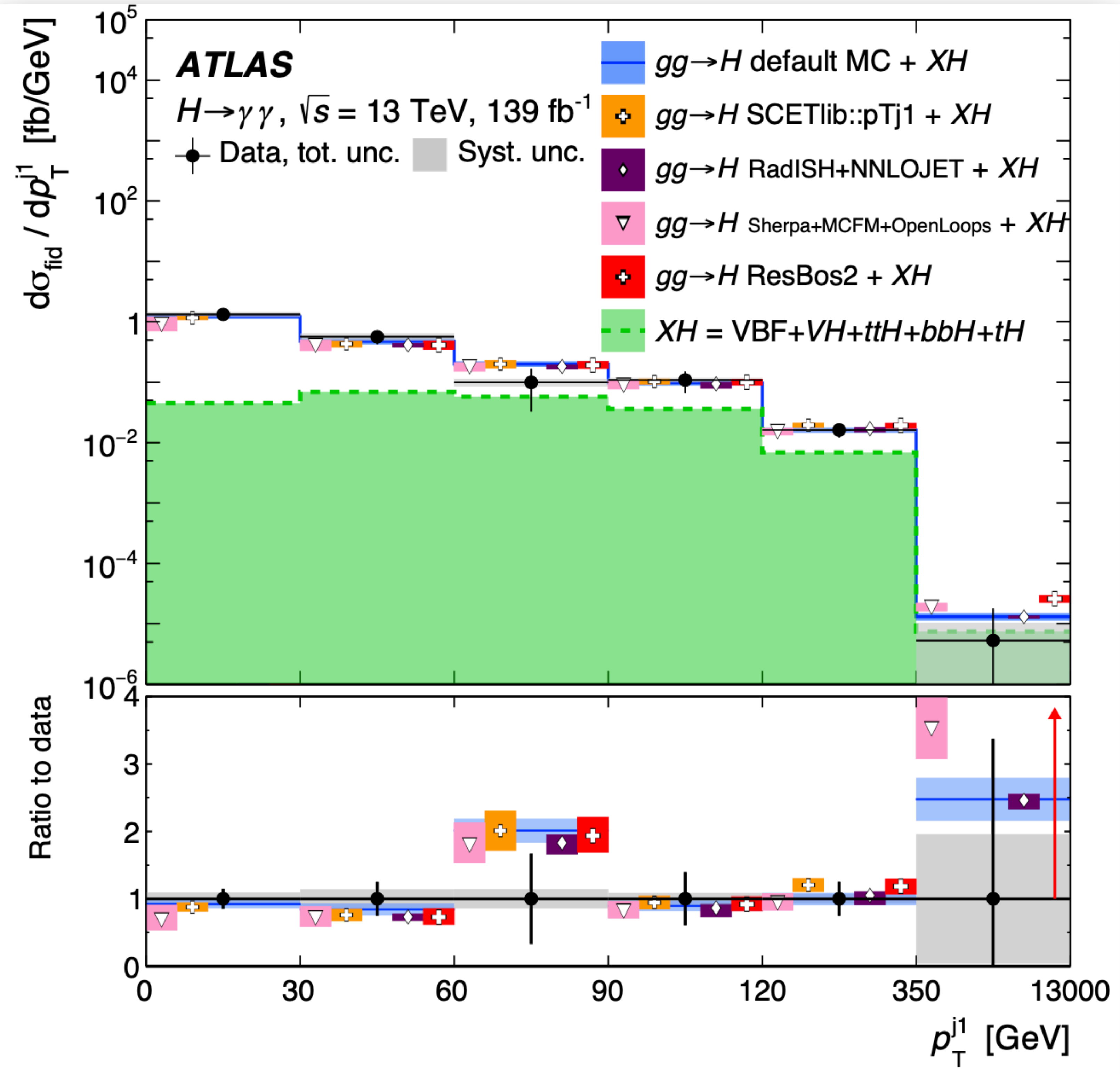

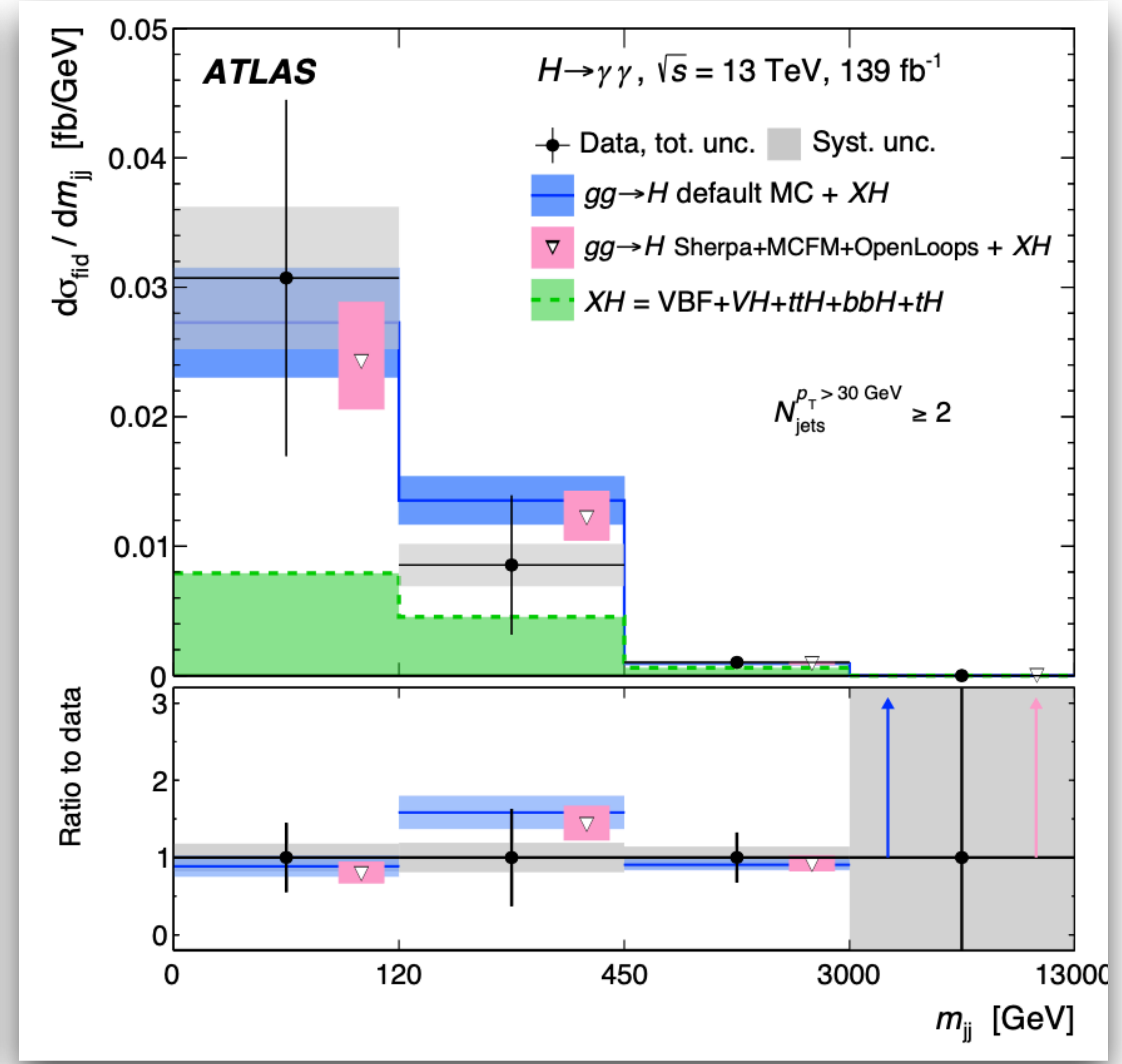

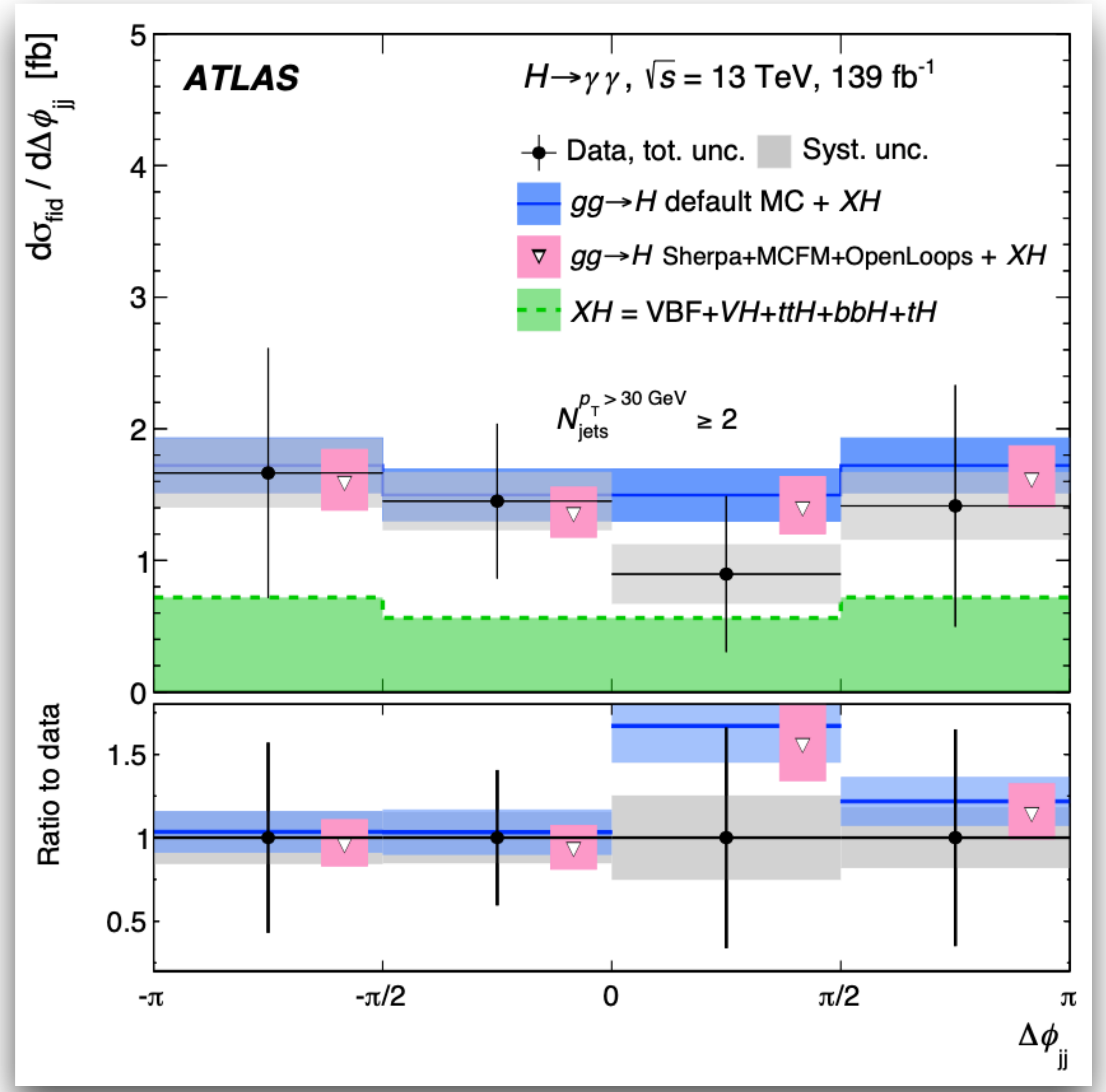

Good agreement with the SM predictions whithin the uncertainties

Double Differential cross-section vs $p_T^{\gamma\gamma}$ vs $|y_{\gamma\gamma}|$ and $p_T^{\gamma\gamma}$ vs $\tau_{C,j1}$

- 2D observables provides further look into the Higgs boson properties and correlations between the observables

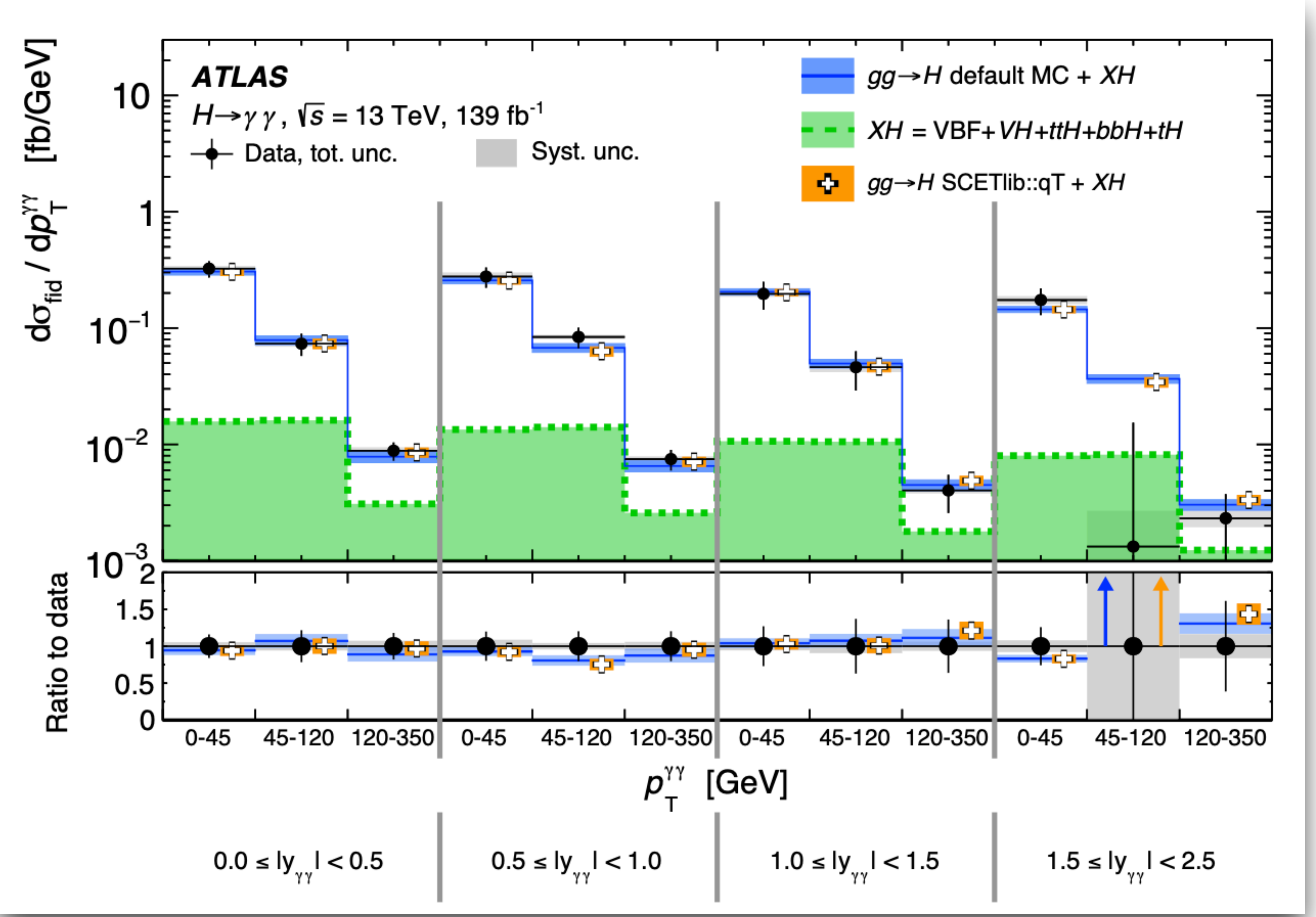

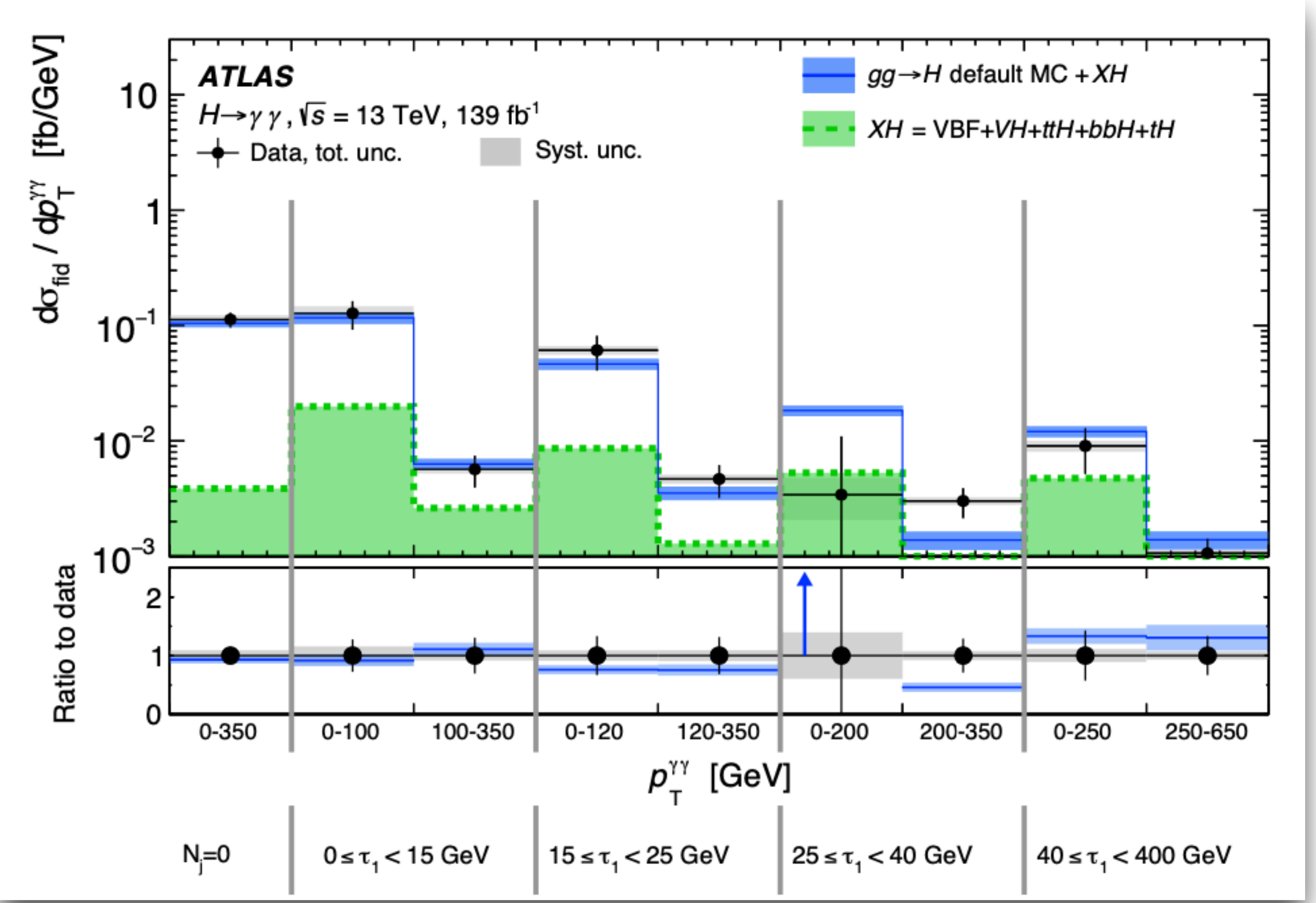

$p_T^{\gamma\gamma}$ vs $|y_{\gamma\gamma}|$
$p(\chi^2)$ = 75% (default MC)

Good agreement with the SM predictions whithin the uncertainties

$p_T^{\gamma\gamma}$ vs $\tau_{C,j1}$
$p(\chi^2)$ = 39% (default MC)

Interpretation using the pT spectrum information

shape only

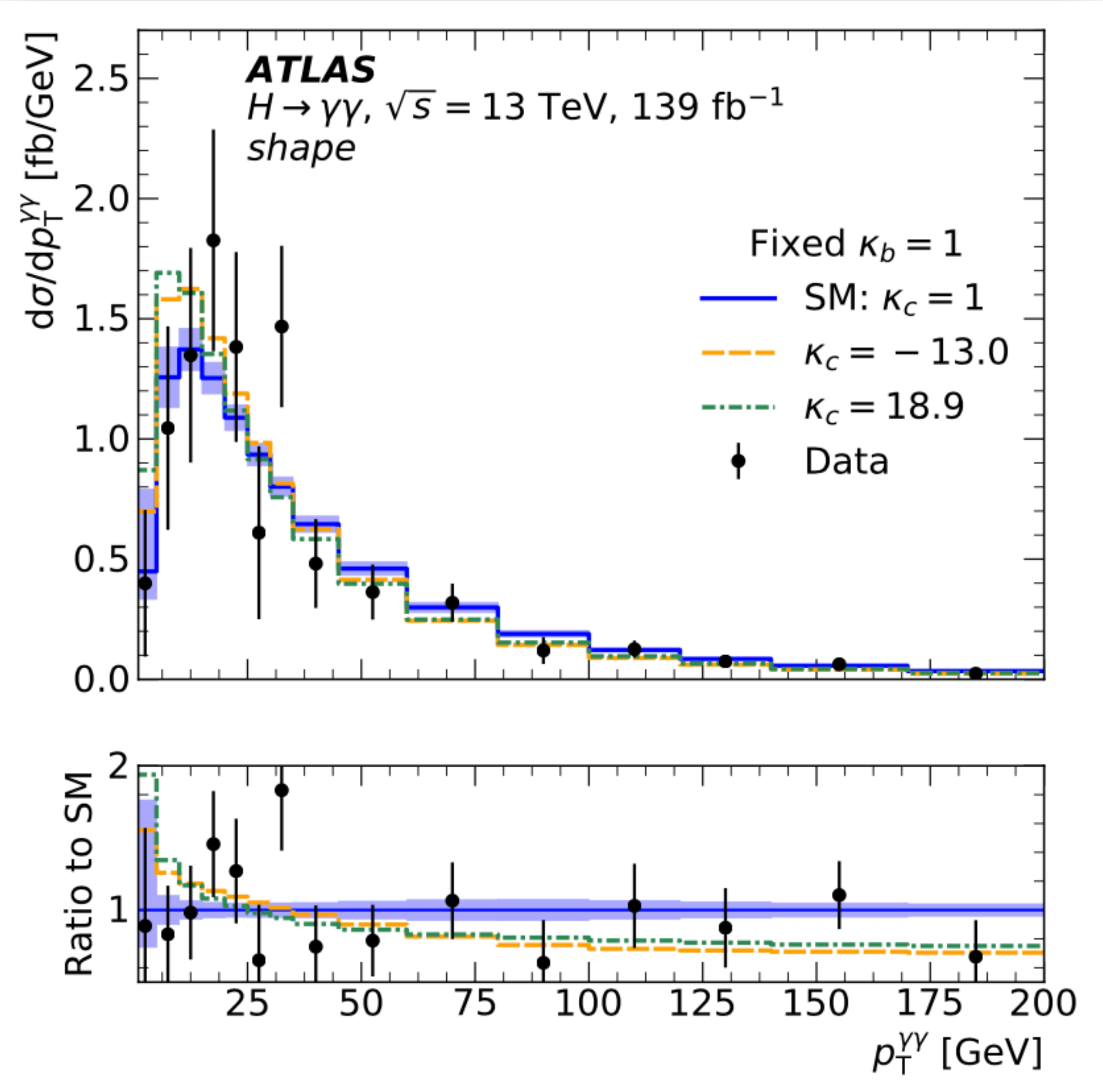

shape+XS+BR

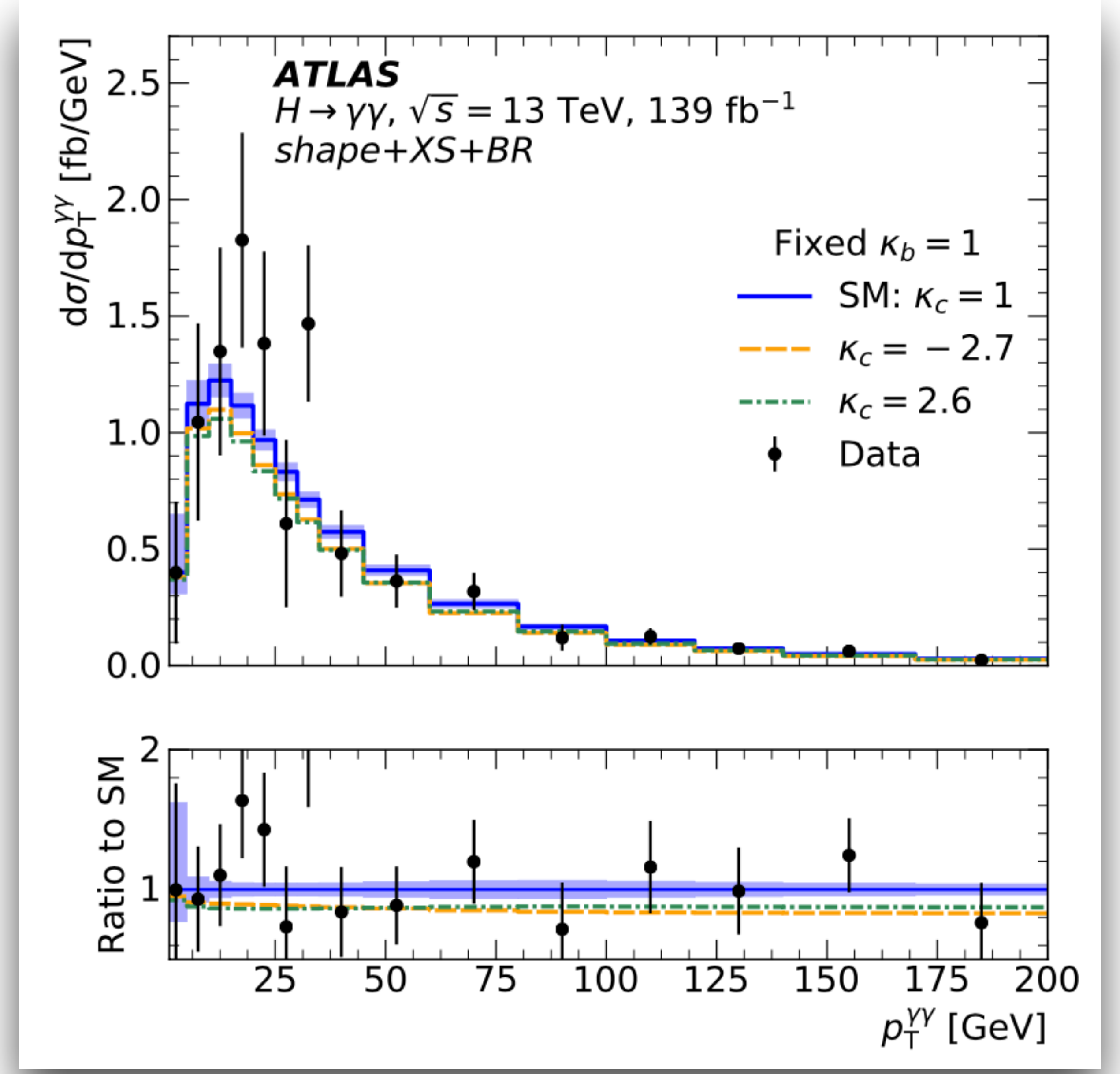

- $p_T^{\gamma\gamma}$ spectrum provides indirect measurement of the c- and b-quarks Yukawa couplings (κ_c and κ_b):
  - shape-only and shape+normalization information are used for the fitting

Fit set-up	κ	Observed 95% CL	Expected 95% CL
Shape-only	κ_c	$[-13.0,\ 18.9]$	$[-10.1,\ 17.3]$
	κ_b	$[-3.7,\ 10.4]$	$[-2.6, 8.1]$
Shape+normalisation (with	κ_c	$[-2.7,\ 2.6]$	$[-3.1,\ 3.2]$
branching ratio variations)	κ_b	$[-1.2,\ -0.8] \cup [0.8,\ 1.1]$	$[-1.2,\ -0.9] \cup [0.8,\ 1.2]$

- Limits on κ_c and κ_b are set from a profile likelihood method:
  - Most sensitive region of $p_T^{\gamma\gamma}$ spectrum < 200 GeV
  - Stronger constraints from shape+normalization
- Shape+normalization constrain on κ_b is comparable to direct searches while κ_c provides stronger constraints (a factor of 3 more stringent for the observed result and a factor of 4 for the expected result)

Direct search limits on κ_c @ 95%CL:
observed: $|\kappa_c| < 8.5$
expected: $|\kappa_c| < 12.4$

Interpretation via Effective Field Theory (EFT)

- **Strength and Tensor structure of the interactions of the Higgs boson:** Effective Field Theory (addition of new interactions CP-even and CP-odd)
  - Constraints derived for the variables: $p_T^{\gamma\gamma}$**, N_jets,** m_{jj}**,** $\Delta\phi_{jj}$ **and** p_T^{j1}
  - BSM contributions probed as non-zero Wilson coefficients
  - Basis of parametrization SMEFT: c_i(CP-even)/$\tilde{c}_i$(CP-odd) (Wilson coefficients); $O_i/\tilde{O}_i$ (6d operators that introduce new interactions)

affect VH/VBF

$$\mathcal{L}_{\text{eff}}^{\text{SMEFT}} \supset c_{HG}O'_g + c_{HW}O'_{HW} + c_{HB}O'_{HB} + c_{HWB}O'_{HWB} + c_{H\tilde{G}}\tilde{O}'_g + c_{H\tilde{W}}\tilde{O}'_{HW} + c_{H\tilde{B}}\tilde{O}'_{HB} + c_{H\tilde{W}B}\tilde{O}'_{HWB}$$

affect $\Delta\phi_{jj}$

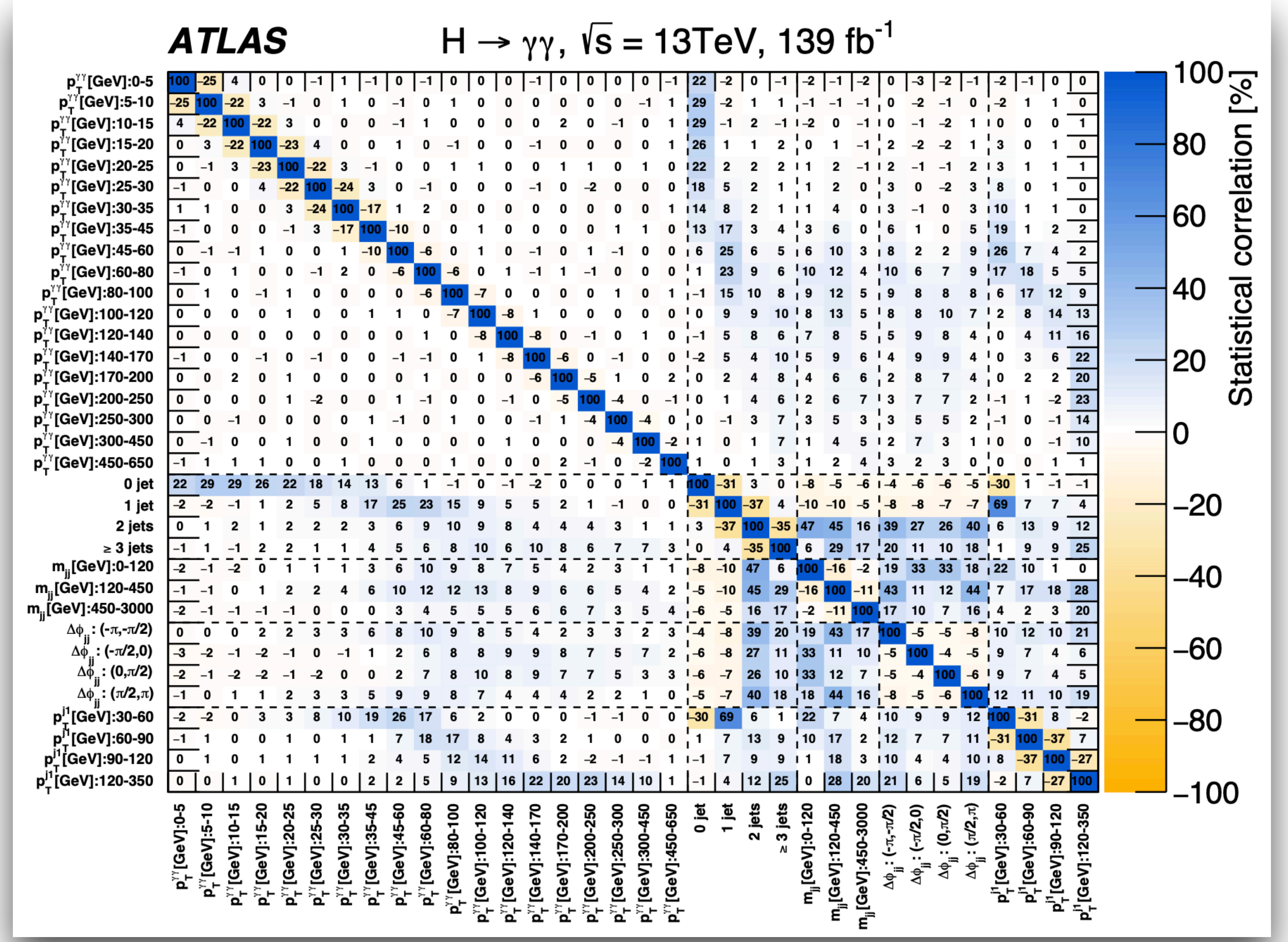

Statistical interpretation:

$$L = \exp\left[-\frac{1}{2}\left(\sigma_{\text{obs}} - \sigma_{\text{pred}}\right)^{\text{T}} C^{-1}\left(\sigma_{\text{obs}} - \sigma_{\text{pred}}\right)\right]$$

- σ_{pred} and σ_{obs} are the k-dimensional vectors from differential cross-section (k = 34, number of bins of the 5 observables distributions)
- C is the covariance matrix: sum of the statistical, systematic and theoretical covariances

interference-terms only

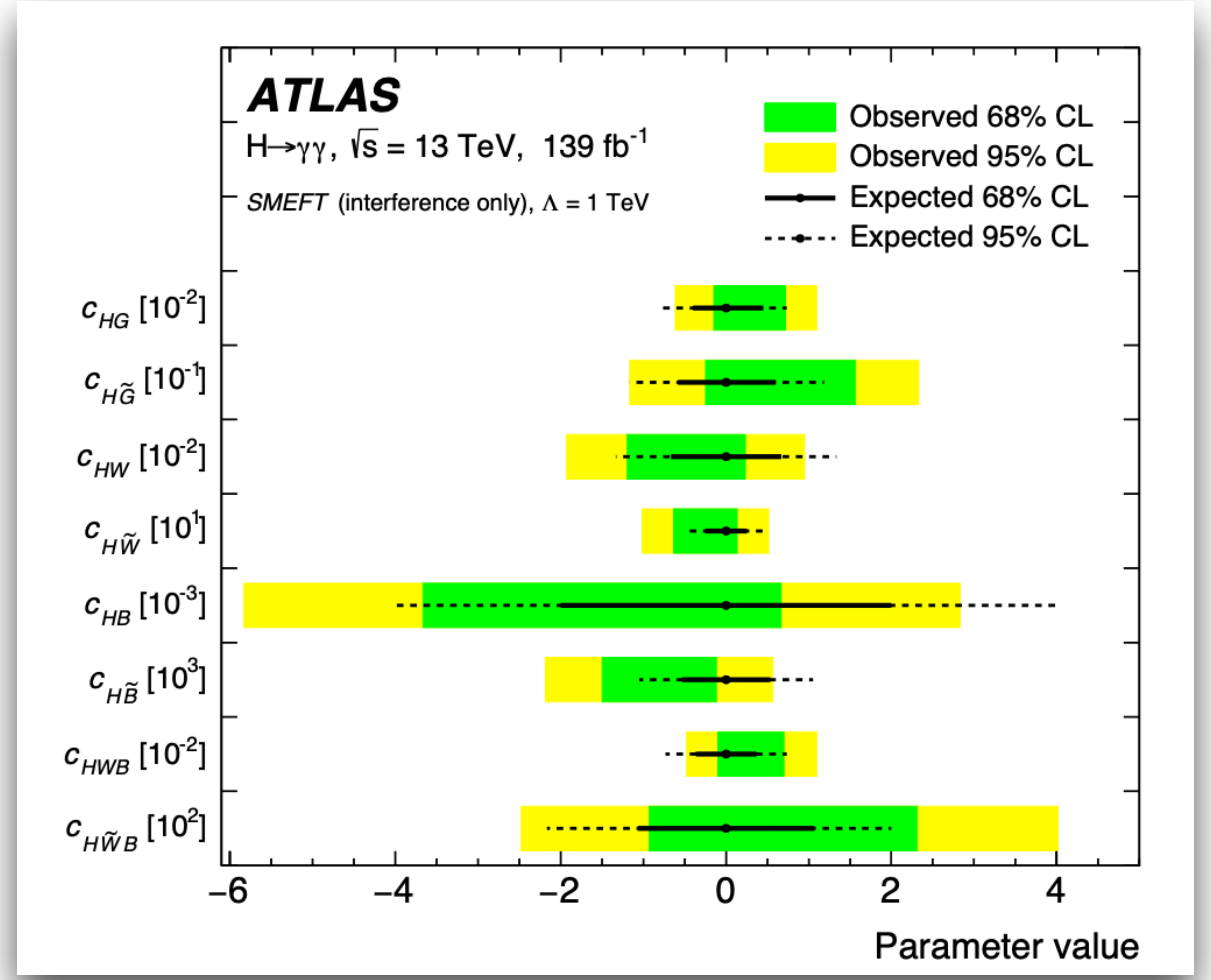

ATLAS and CMS Run2 brief comparisons

- CMS has released a **public result** for the inclusive and differential fiducial cross-section measurements in the diphoton channel using full Run2
- Comparison between the two analysis (diphoton fiducial region):
  - ATLAS/CMS unfolding: matrix response
  - S+B unbinned fit to $m_{\gamma\gamma}$ (ATLAS); S+B binned fit to $m_{\gamma\gamma}$ (CMS)
  - Signal Model: Double Sided Crystall Ball (ATLAS); Sum of Gaussians (CMS)
  - Background modelling: from spurious signal studies (ATLAS); Discrete profiling method (CMS)
  - Uncertainties:
    statistical component: ~ 7.0% (similar)
    Systematic component: spurious signal is about 3.8% (ATLAS) and 0%(included in the statistical error) in CMS

ATLAS

Diphoton fiducial cross-section =
$67 \pm 5(stat.) \pm 4(sys.)\ fb$
SM = $64 \pm 4\ fb$

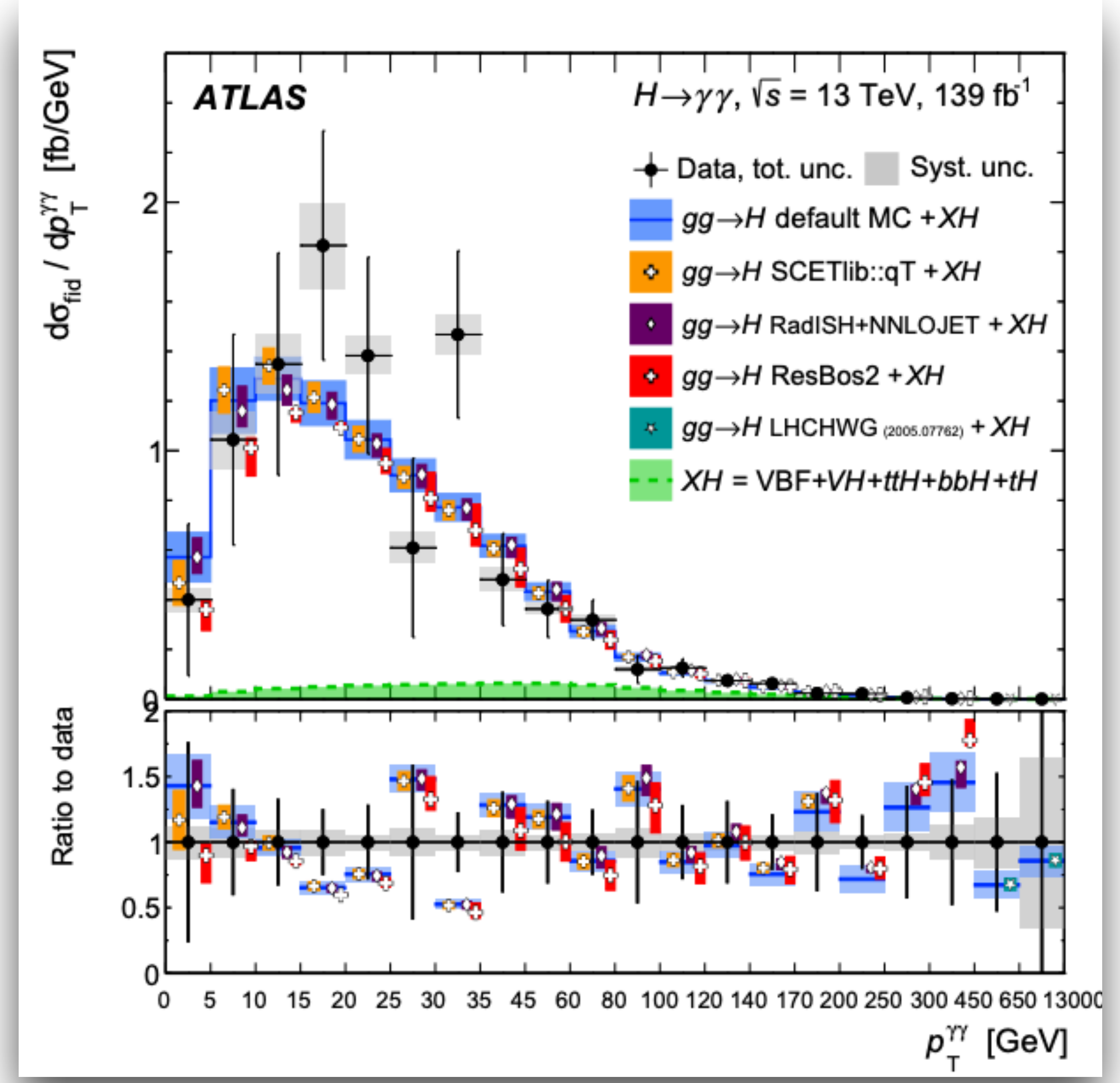

CMS

Diphoton fiducial cross-section =
$73.40^{+6.1}_{-5.9}\ fb$
SM = $75.44 \pm 4.1\ fb$

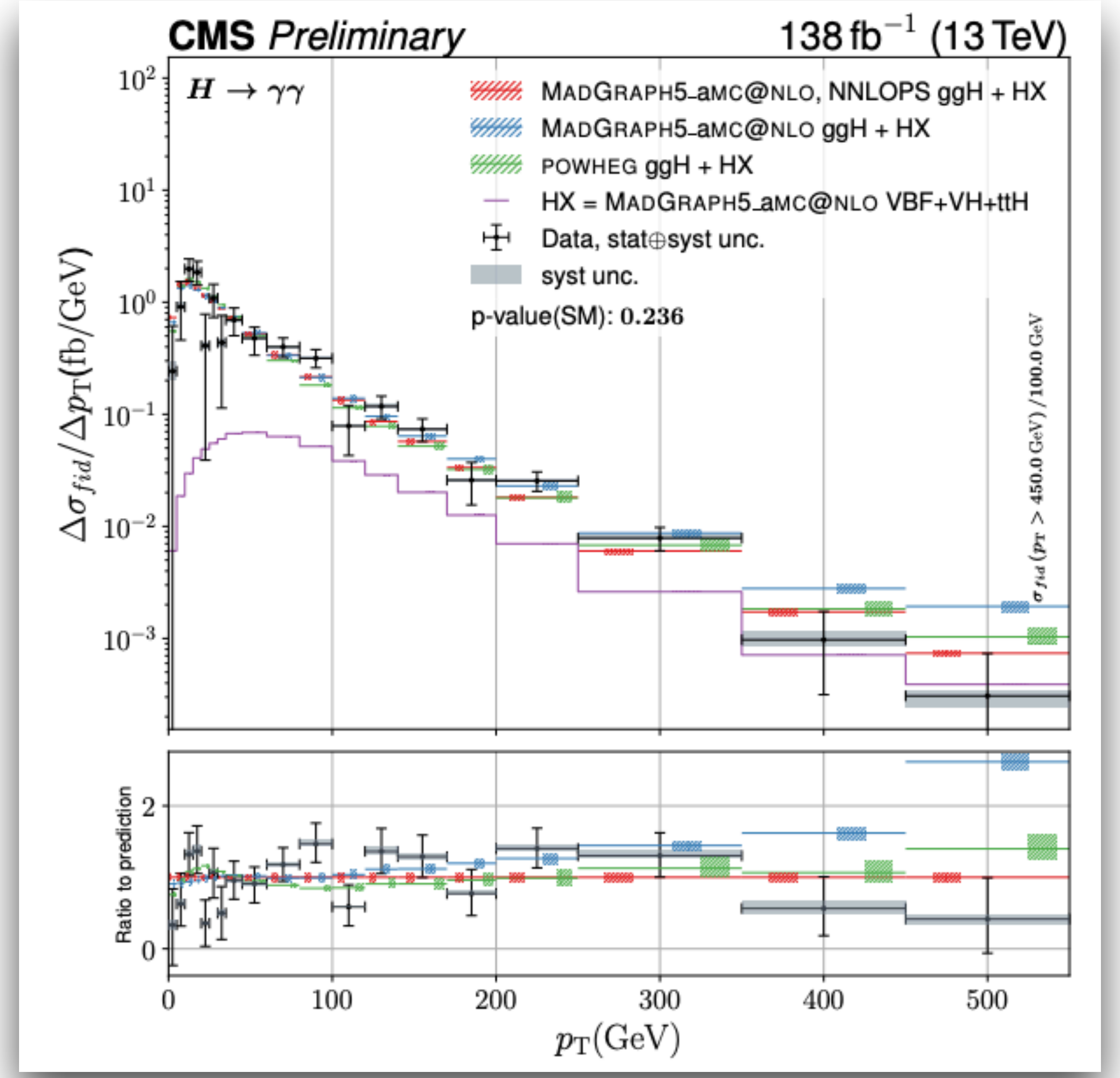

Summary

✓ ***Higgs Fiducial and differential measurements in ATLAS experiment have been presented in the $H \to \gamma\gamma$ channel:***

- Higgs boson properties and probe to new physics contributions in many observables exploring ***Higgs kinematic and jet-kinematic activity in the events***
- ***Very good agreement between the measurements and SM predictions:***
  - Statistical uncertainty still the dominant uncertainty source
- ***Measurements are interpreted in the context of:*** EFT framework and pT(H) shape for bottom- and charm-quark coupling
  - No significant BSM contributions are observed
  - κ_b limits are comparable to the direct searches
  - Stronger limits on κ_c are set compared to direct searches

Stay tuned for Run3 news!

谢谢大家的关注!

Back-up slides

Fraction of signal process in fiducial regions

◉ **Baseline fiducial region (particle level):**

- $E_T/m_{\gamma\gamma} > 0.35$; $E_T/m_{\gamma\gamma} > 0.25$; isolation requirements; $|\eta| < 2.37$ excluding transition region

- **Sub-sets of the baseline fiducial region (sensitive to different Higgs boson production modes):** selections are applied on the electrons, muons, jets and MET

  ◉ **VBF-enchanced region:** at least two jets, $m_{jj} \geq 600 GeV$, $|\Delta y_{jj}| \geq 3.5$

  ◉ $N_{lepton} \geq 1$ **region:** additional charged lepton with pT > 15 GeV. Sensitive to VH (V= W/Z), tH or ttH production modes

  ◉ **High MET region:** large MET > 80 GeV and $p_T^{\gamma\gamma} > 80$ GeV. Sensitive to VH and ttH production mechanisms and BSM effects (WIMPS)

  ◉ **ttH-enchanced region:** at least 1 b-jets/no leptons/4jets or at least 1 lepton and at least 3 jets

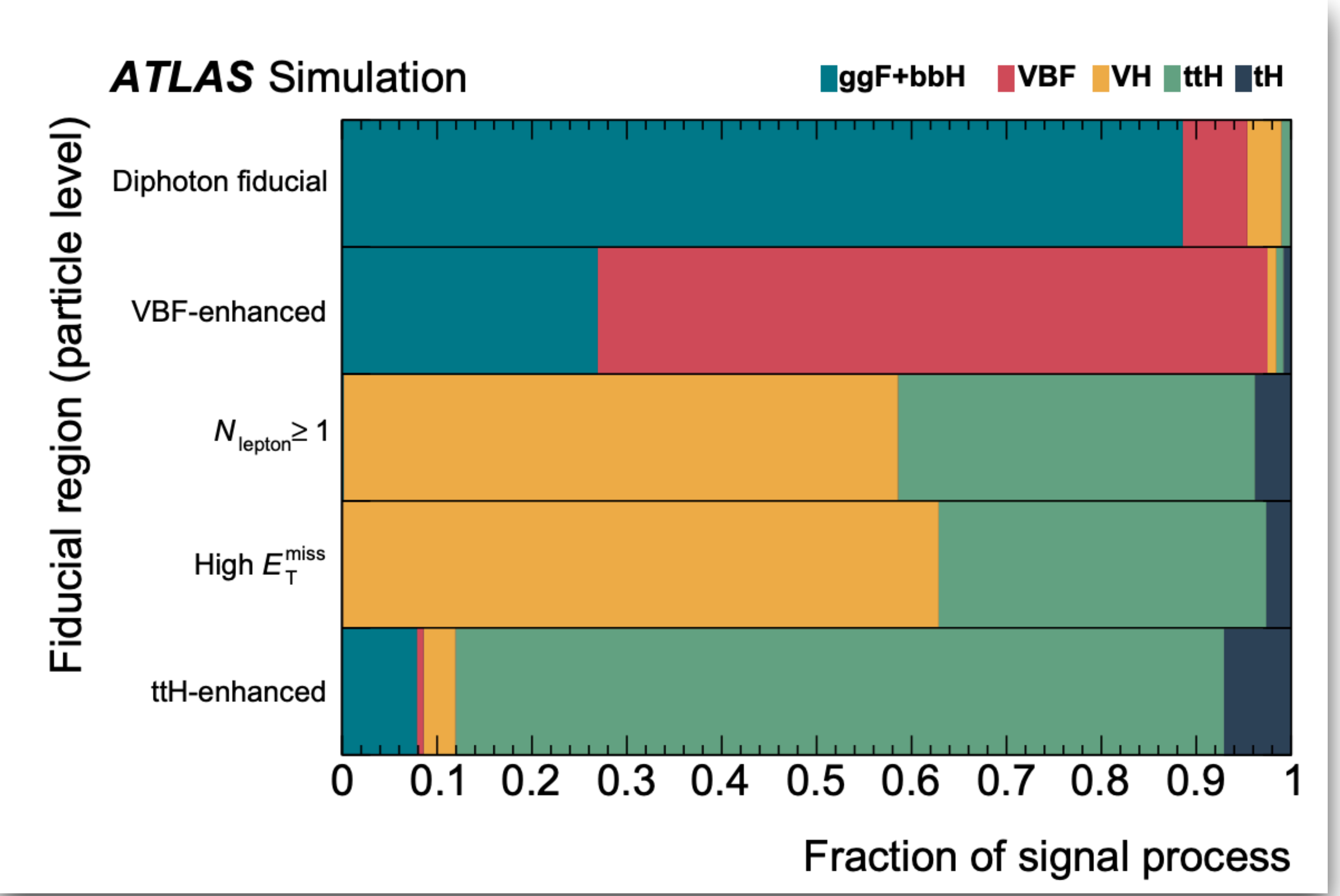

Differential cross-section vs $\tau_{C,j1}$ and $\sum \tau_{C,j}$

$$\tau_{C,j} = \frac{\sqrt{p_T^2 + m^2}}{2cosh(y_j - y_{\gamma\gamma})}$$

m is the jet mass and y_j its rapidity

- Beam-thrust event-shape variable (hadronic observable): boost-invariant along the beam axis
  - $\tau_{C,j1}$ is the highest value of $\tau_{C,j1}$ among all jets in the event while $\sum \tau_{C,j}$ is the scalar sum of τ for all jets with $\tau > 5$ GeV

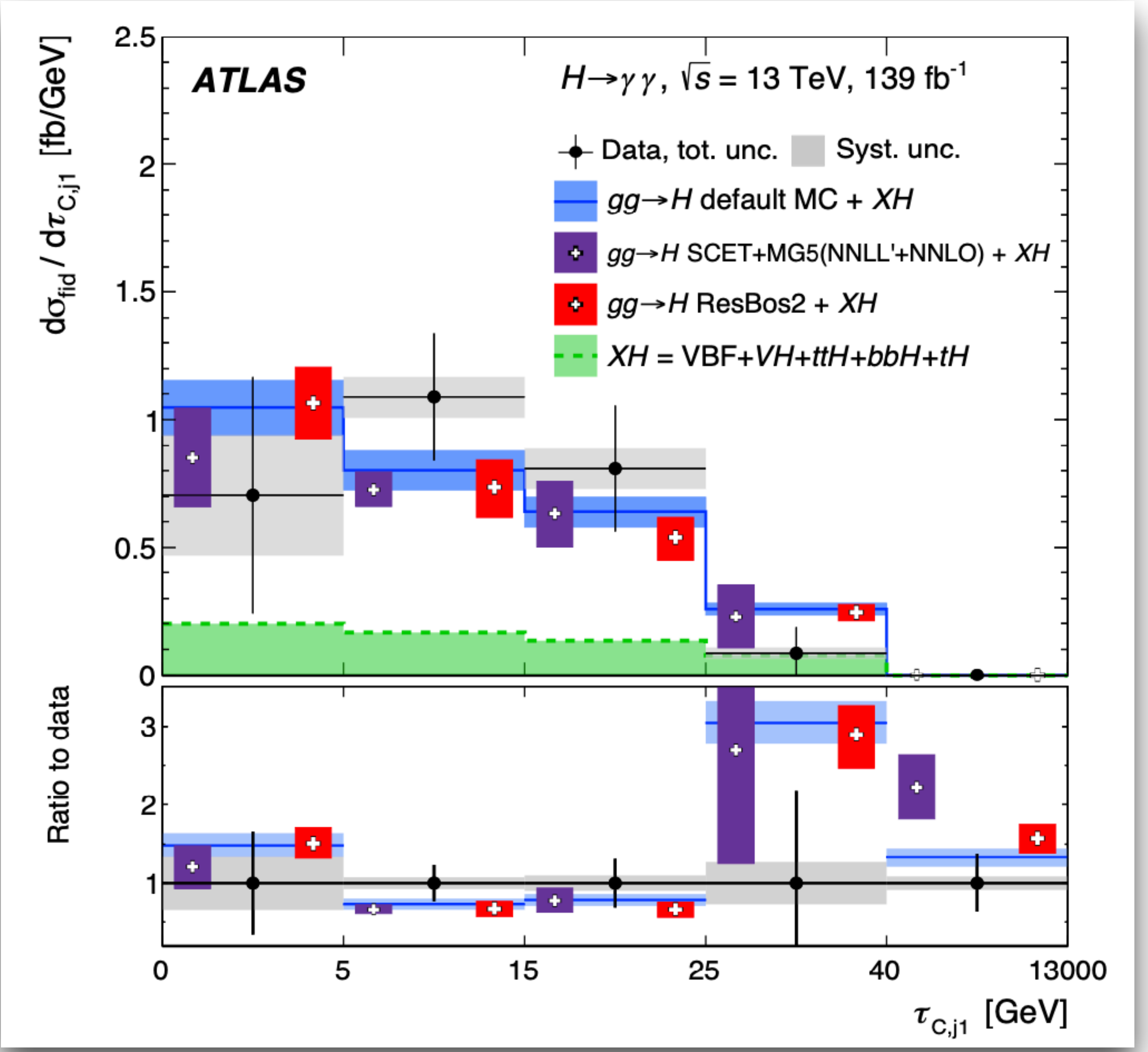

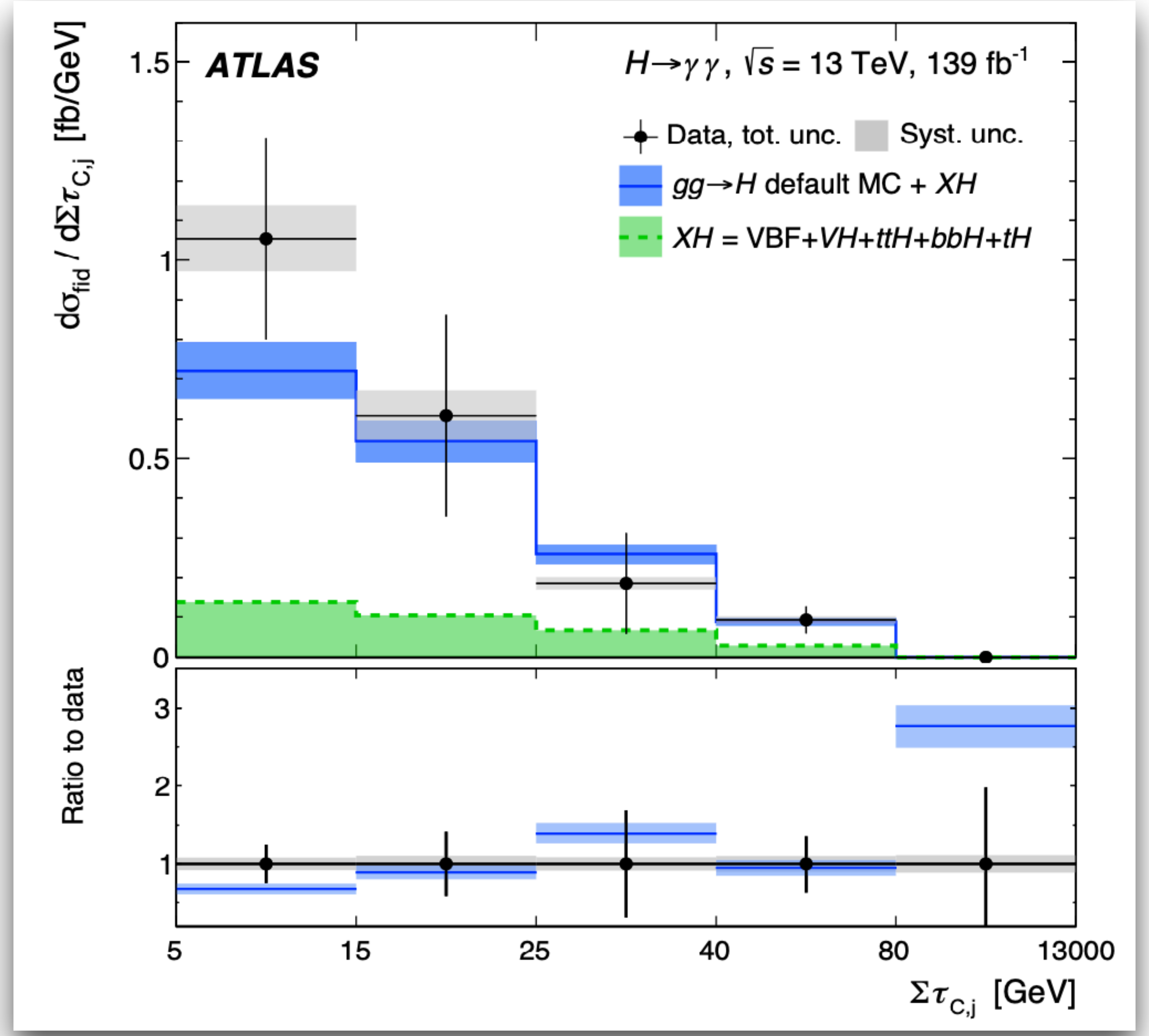

$\tau_{C,j1}$
$p(\chi^2)$ = 27%
(default)

$\sum \tau_{C,j}$
$p(\chi^2)$ = 39%
(default)

Good agreement with the SM predictions

Systematic uncertainties in $p_T^{\gamma\gamma}$ and N_{jets} bins

- Systematics uncertainties sources on the signal and background modeling
- Experimental and theoretical uncertainties uncertainties

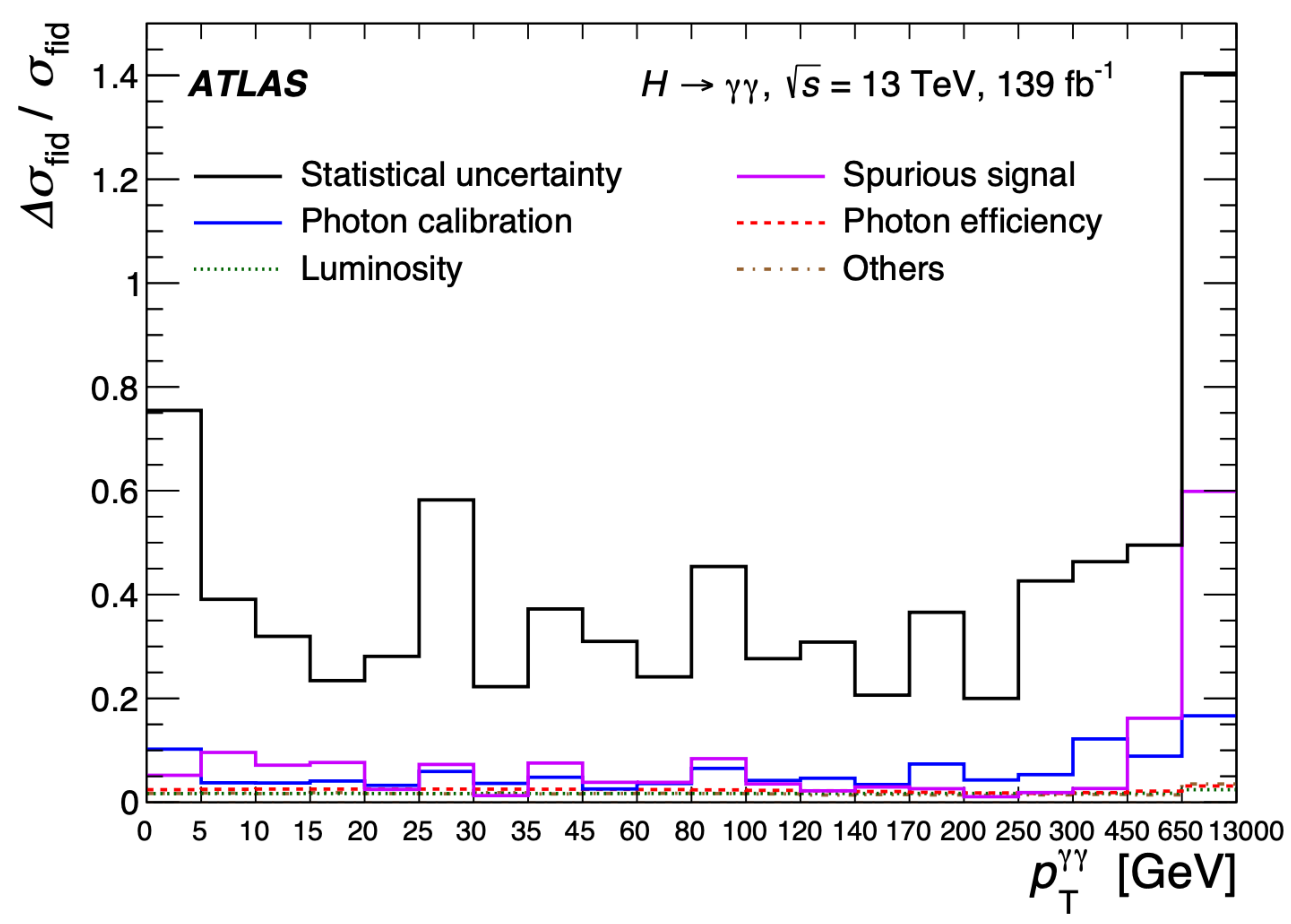

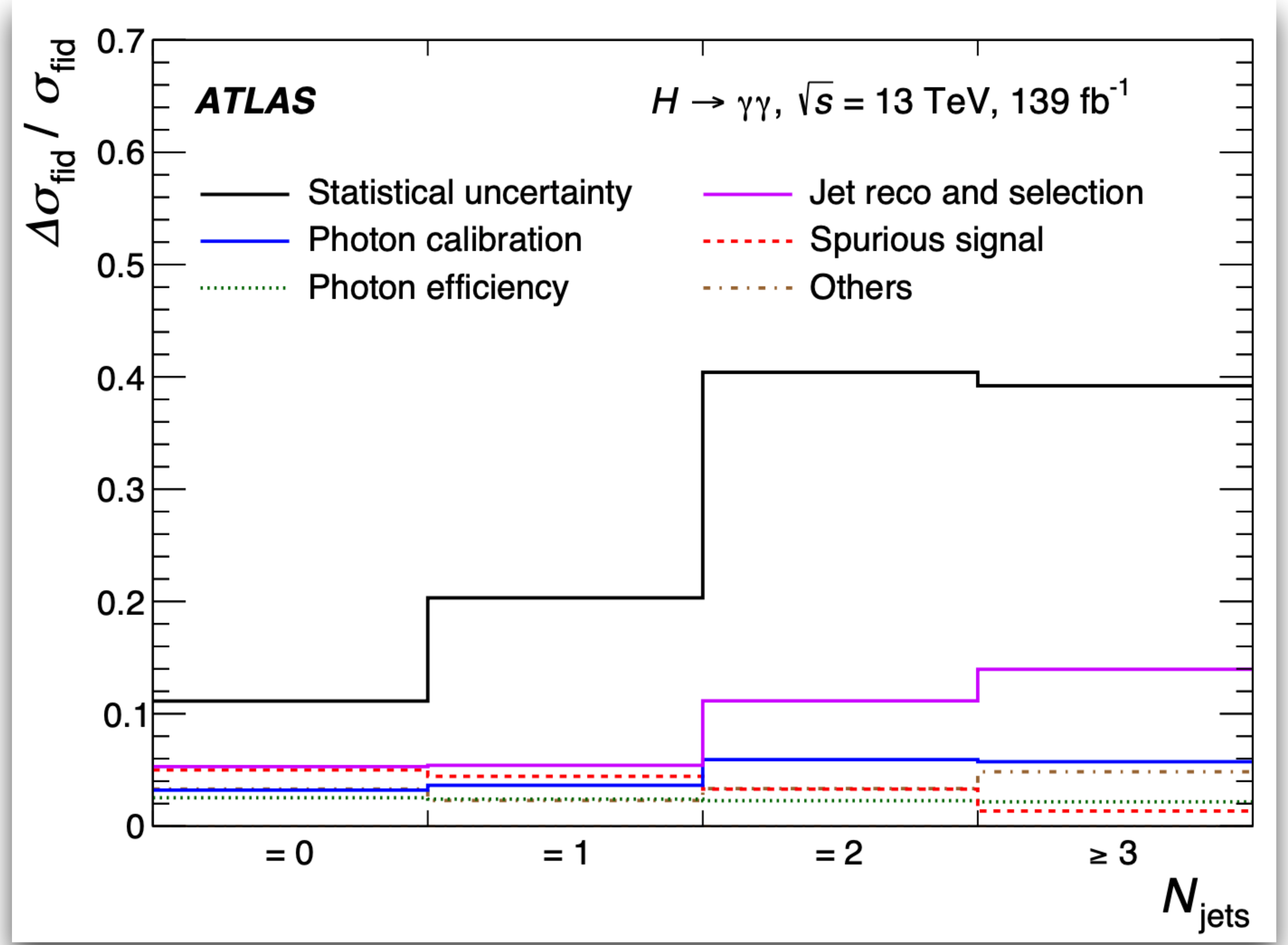

Binning choice for different observables

Variable	Bin Edges	N_{bins}
$p_{\text{T}}^{\gamma\gamma}$	0, 5, 10, 15, 20, 25, 30, 35, 45, 60, 80, 100, 120, 140, 170, 200, 250, 300, 450, 650, 13000	20
$\lvert y_{\gamma\gamma}\rvert$	0, 0.15, 0.3, 0.45, 0.6, 0.75, 0.9, 1.2, 1.6, 2.0, 2.5	10
$p_{\text{T}}^{\gamma 1}/m_{\gamma\gamma}$	0.35, 0.45, 0.5, 0.55, 0.6, 0.65, 0.75, 0.85, 0.95, 10	9
$p_{\text{T}}^{\gamma 2}/m_{\gamma\gamma}$	0.25, 0.35, 0.4, 0.45, 0.5, 0.55, 0.65, 0.75, 0.85, 10	9
N_{jets}	0, 1, 2, ≥ 3	4
$N_{b\text{-jets}}$	$N_{\text{jets}}^{\text{central}} = 0$ or $N_{\text{lep}} > 0$, $N_{b\text{-jets}} = 0, \geq 1$	3
$p_{\text{T}}^{j_1}$	30, 60, 90, 120, 350, 13000	5
H_{T}	30, 60, 140, 200, 500, 13000	5
$p_{\text{T}}^{\gamma\gamma j}$	0, 30, 60, 120, 13000	4
$m_{\gamma\gamma j}$	120, 220, 300, 400, 600, 900, 13000	6
$\tau_{C,j1}$	0, 5, 15, 25, 40, 13000	5
$\sum \tau_{C,j}$	5, 15, 25, 40, 80, 13000	5
$p_{\text{T}}^{\gamma\gamma,\text{ jet veto 30 GeV}}$	0, 5, 10, 15, 20, 30, 40, 50, 100, 13000	9
$p_{\text{T}}^{\gamma\gamma,\text{ jet veto 40 GeV}}$	0, 5, 10, 15, 20, 30, 40, 50, 60, 100, 13000	10
$p_{\text{T}}^{\gamma\gamma,\text{ jet veto 50 GeV}}$	0, 5, 10, 15, 20, 30, 40, 50, 60, 70, 100, 13000	11
$p_{\text{T}}^{\gamma\gamma,\text{ jet veto 60 GeV}}$	0, 5, 10, 15, 20, 30, 40, 50, 60, 70, 80, 100, 13000	12
m_{jj}	0, 120, 450, 3000, 13000	4
$\Delta\phi_{jj}$	$-\pi, -\frac{\pi}{2}, 0, \frac{\pi}{2}, \pi$	4
$\pi - \lvert\Delta\phi_{\gamma\gamma,jj}\rvert$	0, 0.15, 0.65, π	3
$p_{\text{T},\gamma\gamma jj}$	0, 30, 60, 120, 13000	4
VBF-enhanced: $p_{\text{T}}^{j_1}$	30, 120, 13000	2
VBF-enhanced: $\Delta\phi_{jj}$	$-\pi, -\frac{\pi}{2}, 0, \frac{\pi}{2}, \pi$	4
VBF-enhanced: $\lvert\eta^*\rvert$	0, 1, 2, 10	3
VBF-enhanced: $p_{\text{T},\gamma\gamma jj}$	0, 30, 13000	2

Binning choice for different observables

Variable	Bin Edges		N_{bins}
$p_{\text{T}}^{\gamma\gamma}$ vs $\lvert y_{\gamma\gamma}\rvert$	$0.0 < \lvert y_{\gamma\gamma}\rvert < 0.5$	$p_{\text{T}}^{\gamma\gamma}$: 0, 45, 120, 350	12
	$0.5 < \lvert y_{\gamma\gamma}\rvert < 1.0$	$p_{\text{T}}^{\gamma\gamma}$: 0, 45, 120, 350	
	$1.0 < \lvert y_{\gamma\gamma}\rvert < 1.5$	$p_{\text{T}}^{\gamma\gamma}$: 0, 45, 120, 350	
	$1.5 < \lvert y_{\gamma\gamma}\rvert < 2.5$	$p_{\text{T}}^{\gamma\gamma}$: 0, 45, 120, 350	
$(p_{\text{T}}^{\gamma1} + p_{\text{T}}^{\gamma2})/m_{\gamma\gamma}$ vs $(p_{\text{T}}^{\gamma1} - p_{\text{T}}^{\gamma2})/m_{\gamma\gamma}$	$0.6 < (p_{\text{T}}^{\gamma1} + p_{\text{T}}^{\gamma2})/m_{\gamma\gamma} \leq 0.8$	$(p_{\text{T}}^{\gamma1} - p_{\text{T}}^{\gamma2})/m_{\gamma\gamma}$: 0, 0.3	8
	$0.8 < (p_{\text{T}}^{\gamma1} + p_{\text{T}}^{\gamma2})/m_{\gamma\gamma} \leq 1.1$	$(p_{\text{T}}^{\gamma1} - p_{\text{T}}^{\gamma2})/m_{\gamma\gamma}$: 0, 0.05, 0.1, 0.2, 0.8	
	$1.1 < (p_{\text{T}}^{\gamma1} + p_{\text{T}}^{\gamma2})/m_{\gamma\gamma} \leq 4$	$(p_{\text{T}}^{\gamma1} - p_{\text{T}}^{\gamma2})/m_{\gamma\gamma}$: 0, 0.3, 0.6, 4	
$p_{\text{T}}^{\gamma\gamma}$ vs $p_{\text{T}}^{\gamma\gamma j}$	$N_{\text{jets}} = 0$	$p_{\text{T}}^{\gamma\gamma}$: 0, 350	9
	$0 < p_{\text{T}}^{\gamma\gamma j} \leq 30$	$p_{\text{T}}^{\gamma\gamma}$: 0, 100, 350	
	$30 < p_{\text{T}}^{\gamma\gamma j} \leq 60$	$p_{\text{T}}^{\gamma\gamma}$: 0, 45, 120, 350	
	$60 < p_{\text{T}}^{\gamma\gamma j} \leq 350$	$p_{\text{T}}^{\gamma\gamma}$: 0, 80, 250, 450	
$p_{\text{T}}^{\gamma\gamma}$ vs $\tau_{C,j1}$	$N_{\text{jets}} = 0$	$p_{\text{T}}^{\gamma\gamma}$: 0, 350	9
	$0 < \tau_{C,j1} \leq 15$	$p_{\text{T}}^{\gamma\gamma}$: 0, 100, 350	
	$15 < \tau_{C,j1} \leq 25$	$p_{\text{T}}^{\gamma\gamma}$: 0, 120, 350	
	$25 < \tau_{C,j1} \leq 40$	$p_{\text{T}}^{\gamma\gamma}$: 0, 200, 350	
	$40 < \tau_{C,j1} \leq 400$	$p_{\text{T}}^{\gamma\gamma}$: 0, 250, 650	
VBF-enhanced: $p_{\text{T}}^{j_1}$ vs $\Delta\phi_{jj}$	$-\pi < \Delta\phi_{jj} < 0$	$p_{\text{T}}^{j_1}$: 30, 120, 500	4
	$0 < \Delta\phi_{jj} < \pi$	$p_{\text{T}}^{j_1}$: 30, 120, 500	

S+B fits to $m_{\gamma\gamma}$ in different fiducial regions

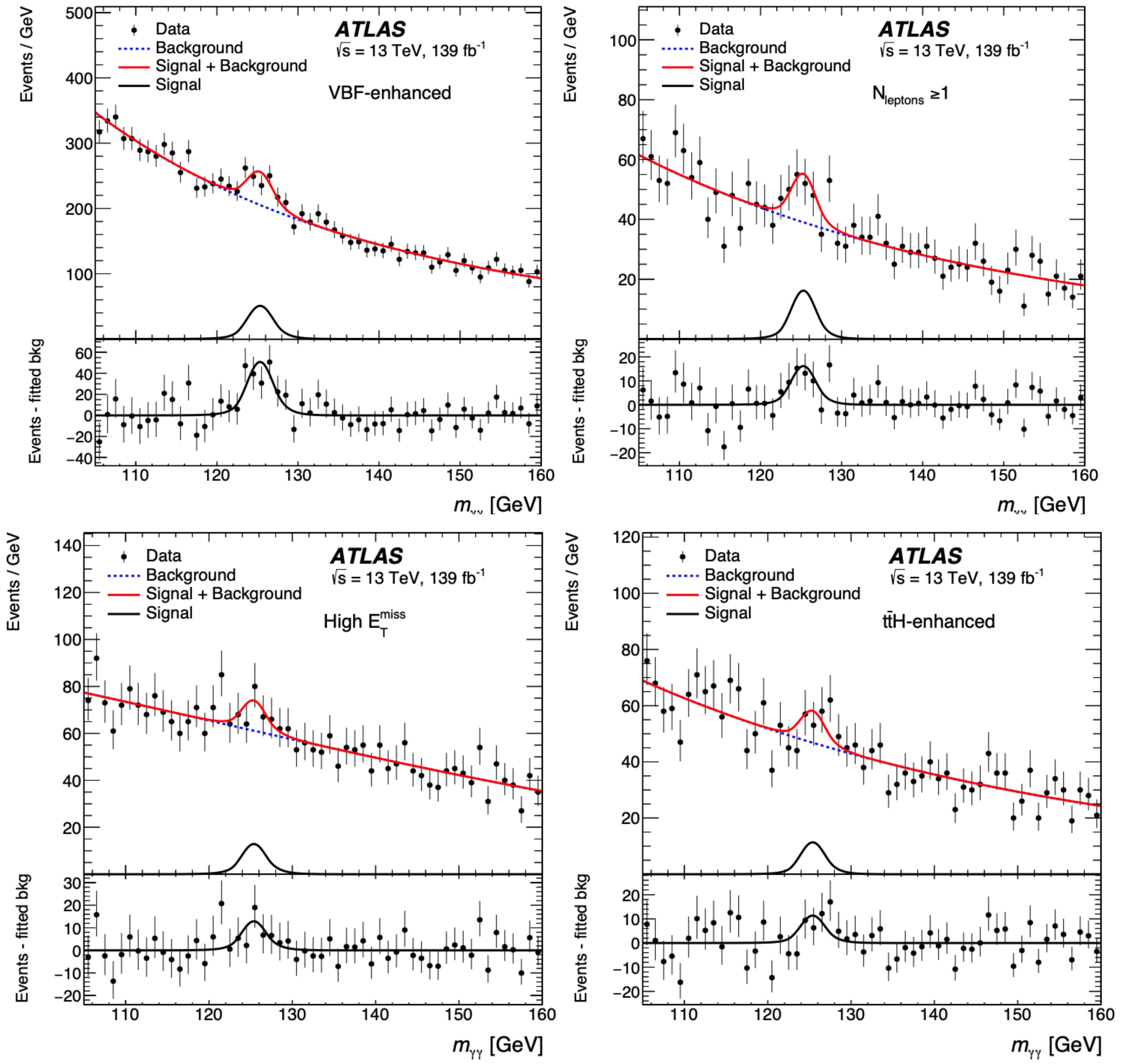

χ^2 test is used to evaluate the p-value compatibility between the measurements and SM predictions

Fiducial region	Measured [fb]					SM prediction [fb]			95% CL$_s$ upper limit [fb]	p-value
		±	stat	±	sys					
Diphoton	67	±	5	±	4	64	±	4	-	69%
VBF-enhanced	1.8	±	0.5	±	0.3	1.53	±	0.10	-	64%
$N_{\text{lepton}} \geq 1$	0.81	±	0.23	±	0.06	0.59	±	0.03	-	36%
High E_T^{miss}	0.28	±	0.27	±	0.07	0.302	±	0.017	0.85	93%
$t\bar{t}H$-enhanced	0.53	±	0.27	±	0.06	0.60	±	0.05	1.13	79%
Total	132	±	10	±	8	126	±	7	-	69%

χ^2 computation includes full uncertainties in fitted cross-section and theory uncertainties from SM predictions

Response matrices for $p_T^{\gamma\gamma}$ and N_{jets} bins

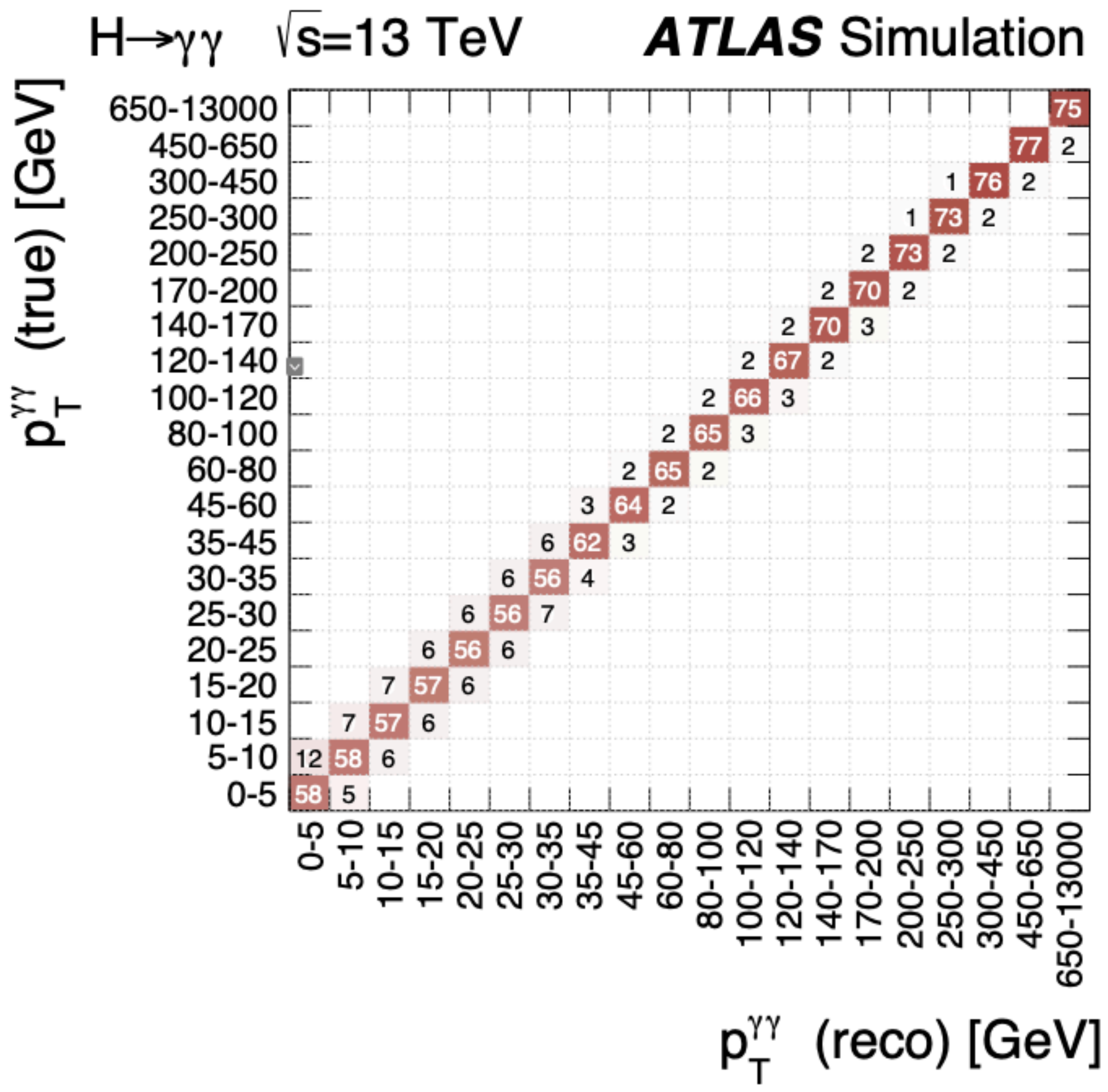

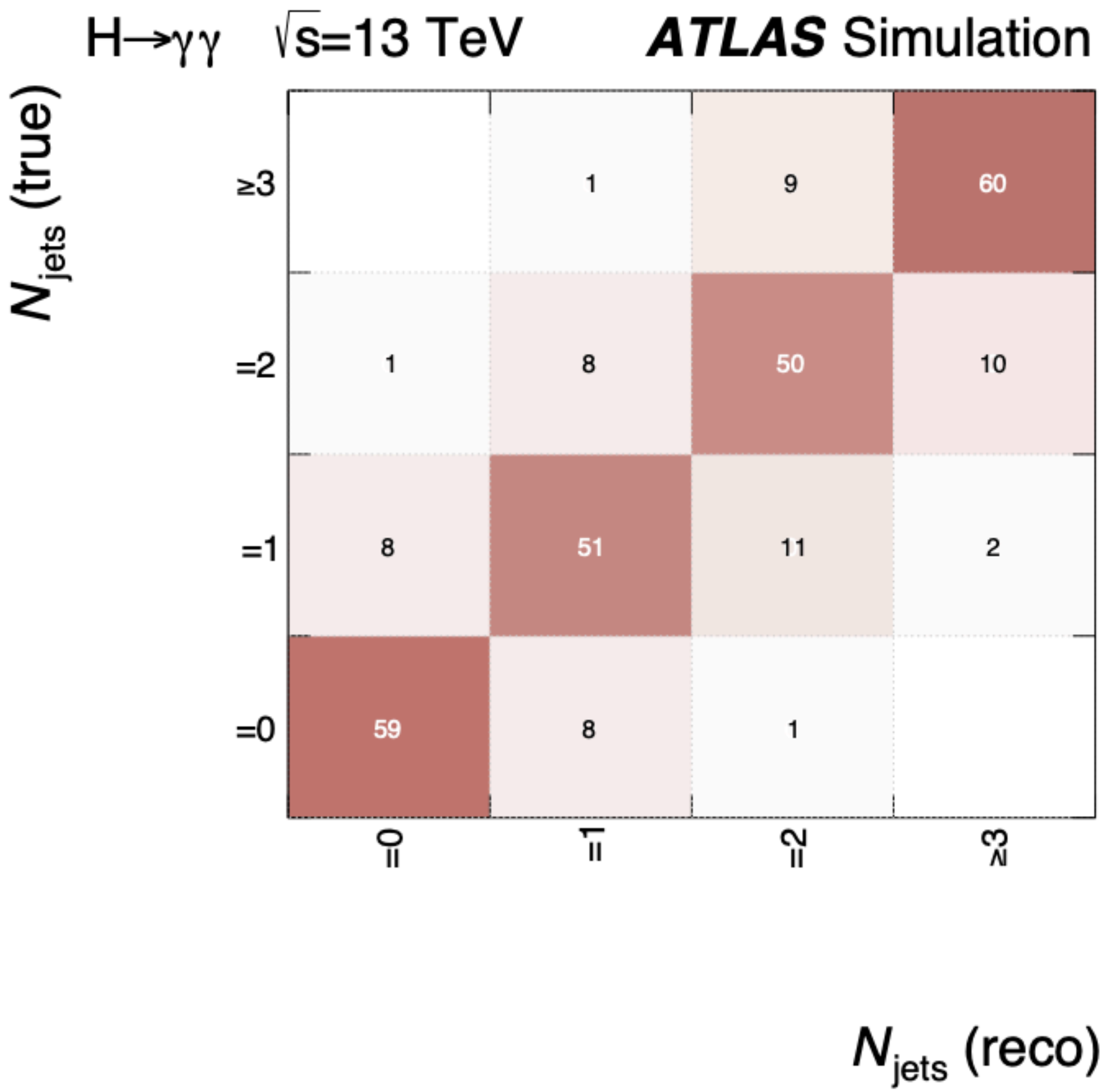

p-values: measured/predicted cross-sections

Variable	p-value										
	default	RadISH NNLOJET	NNLOJet	STWZ BLPTW	MATRIX	SHERPA	GoSam	SCETlib	TAUC	ResBos2	proVBF
$p_T^{\gamma 1}/m_{\gamma\gamma}$	56%	–	–	–	–	–	–	58%	–	32%	–
$p_T^{\gamma 2}/m_{\gamma\gamma}$	93%	–	–	–	–	–	–	49%	–	2%	–
$p_T^{\gamma\gamma}$	86%	68%	–	–	–	–	–	78%	–	54%	–
$\lvert y_{\gamma\gamma}\rvert$	76%	–	–	–	–	–	–	78%	–	66%	–
$p_T^{j_1}$	78%	77%	–	–	–	47%	–	48%	–	38%	–
N_{jets}	95%	–	90%	56%	–	59%	84%	–	–	–	–
$N_{b\text{-jets}}$	60%	–	–	–	–	–	–	–	–	–	–
$p_T^{\gamma\gamma j}$	81%	–	–	–	–	68%	–	–	–	78%	–
$m_{\gamma\gamma j}$	95%	–	–	–	–	95%	–	–	–	–	–
$\tau_{C,j1}$	27%	–	–	–	–	–	–	–	11%	13%	–
$\sum \tau_{C,j}$	39%	–	–	–	–	–	–	–	–	–	–
H_T	46%	–	–	–	–	51%	–	–	–	–	–
m_{jj}	79%	–	–	–	–	81%	–	–	–	–	–
$\Delta\phi_{jj}$	91%	–	–	–	–	95%	–	–	–	–	–
$\lvert\Delta\phi_{\gamma\gamma,jj}\rvert$	83%	–	–	–	–	88%	–	–	–	–	–
$p_{T,\gamma\gamma jj}$	99%	–	–	–	–	100%	–	–	–	–	–
$p_T^{\gamma\gamma}$ jetveto 30 GeV	84%	–	–	–	83%	–	–	–	–	83%	–
$p_T^{\gamma\gamma}$ jetveto 40 GeV	95%	–	–	–	45%	–	–	–	–	83%	–
$p_T^{\gamma\gamma}$ jetveto 50 GeV	88%	–	–	–	35%	–	–	–	–	30%	–
$p_T^{\gamma\gamma}$ jetveto 60 GeV	67%	–	–	–	52%	–	–	–	–	42%	–
$p_T^{\gamma\gamma}$ vs $\lvert y_{\gamma\gamma}\rvert$	75%	–	–	–	–	–	–	78%	–	–	–
$p_T^{\gamma\gamma}$ vs $\tau_{C,j1}$	39%	–	–	–	–	–	–	–	–	–	–
$p_T^{\gamma\gamma}$ vs $p_T^{\gamma\gamma j}$	96%	–	–	–	–	–	–	–	–	–	–
$(p_T^{\gamma 1} - p_T^{\gamma 2})/m_{\gamma\gamma}$ vs $(p_T^{\gamma 1} + p_T^{\gamma 2})/m_{\gamma\gamma}$	81%	–	–	–	–	–	–	77%	–	–	–
VBF $\lvert\eta^*\rvert$	94%	–	–	–	–	–	–	–	–	–	70%
VBF $\Delta\phi_{jj}$	68%	–	–	–	–	–	–	–	–	–	65%
VBF $p_T^{j_1}$	77%	–	–	–	–	–	–	–	–	–	70%
VBF $p_{T,\gamma\gamma jj}$	89%	–	–	–	–	–	–	–	–	–	74%
VBF $p_T^{j_1}$ vs $\Delta\phi_{jj}$	76%	–	–	–	–	–	–	–	–	–	74%